INSTITUTO TECNOLÓGICO DE COSTA RICA

VICERRECTORÍA DE INVESTIGACIÓN Y EXTENSIÓN

DIRECCIÓN DE PROYECTOS

ESCUELA DE INGENIERÍA FORESTAL

CENTRO DE INVESTIGACIÓN EN INNOVACION FORESTAL

INFORME FINAL DE PROYECTO DE INVESTIGACIÓN

Aplicación de nanocelulosa de una fuente lignocelulósica (mata de piña) en el reforzamiento de un producto compuesto de madera.

(DOCUMENTO I)

INVESTIGADORES:

Roger Moya R, Ph.D.
Ricardo Starbird P. Ph.D.
Angel Navarro M., Lic.
Johana Gaitán Á., MSc.
.

Diciembre, 2018

ÍNDICE GENERAL

Pág.

RESUMEN DE RESULTADOS POR OBJECTIVOS

Objetivo especifico	Resultados
1. Establecer un protocolo de extracción de nanocelulosa de desechos de piña y caracterizarla acorde a las técnicas de nano-observación	El tallo de la piña húmeda es cortado a un tamaño de 2 cm y secado a 80 °C hasta alcanzar una humedad del 4%. Luego es triturado a un tamaño de 300 µm. Se prepara una solución de con hidróxido de sodio (NaOH) a 2.5% y se verte en la piña triturada. Luego se calienta a una temperatura de 100°C por un periodo de 4h. Luego el material es lavado con agua destilada hasta obtener un pH neutro, para su posterior blanqueamiento con hipoclorito de sodio (NaClO) a una concentración de 4% durante un periodo de 2 h. Seguidamente el material se lava con agua destilada hasta alcanzar un pH neutro (Rambabu et al., 2016). Luego la nanocelulosa es obtenida por reacción de hidrólisis química haciendo uso de una disolución de ácido clorhídrico (HCl) de concentración 2.5 N, utilizando un sistema de reflujo a una temperatura de 90°C por un periodo de 30 min para su posterior filtración y neutralización con agua destilada (Gaspar et al., 2014). *Extracción de nanocelulosa cristalina:* Este procedimiento consistió en el tratamiento de la nanocelulosa con ácido sulfúrico (H_2SO_4) al 64% a temperatura ambiente y por periodo de1h. Mediante diálisis se llevó a un pH entre 3-5 y por tratamiento mecánico mediante uso de un ultrasónico (Amplitud 70, tiempo 10min) se obtuvo el hidrogel de nanocelulosa (0.033g ml^{-1}, m v^{-1}).
2. Establecer el protocolo para incorporar la nanocelulosa en los dos adhesivos para madera, y obtener sus efectos en la propiedades de resistencia de la línea de cola en la madera	En dos tipos de adhesivos para madera, PVAc y UF, fue agregado nanocelulosa en tres concentraciones: 0% (control), 0.5% y 1.0% (peso $peso^{-1}$), la cual fue añadida con base en el porcentaje de sólidos de cada adhesivo (55% para PVAc y 48% para UF. La mezcla de la nanocelulosa con los adhesivos se prepara de la siguiente forma: en el caso del PVAc, es tomado 150 gramos y colocada en un recipiente y puesto a agitar con ayuda de un agitador de cuchillas inclinadas con aspas de 45° a 1600 rpm. Luego se toma la proporción de MNCC en gel (aproximadamente 13.75 ml para la concentración 0.5% y 27.5 ml para la concentración del 1.0% y se va agregando lentamente al adhesivo. Una vez que se mezcla la nanocelulosa en el adhesivo, se mantiene la agitación durante 10 minutos. Mientras que para UF, por tratarse de 4 componentes (resina, agua, harina y sulfato de amonio como catalizador), 76.5 g de la resina es mezclada con 12 ml y 24 ml para las concentraciones de 0.5% y 1.0%, respectivamente de MNCC. Esta mezcla es agitada durante 5 minutos a 1600 rpm con ayuda de un agitador de cuchillas inclinadas, luego se añade los demás componentes (27-15 ml restantes de agua, 30 g harina y 4.5 ml de catalizador) y se continua la agitación durante 5 minutos adicionales.
3. Desarrollar un producto para cada tipo de adhesivo basados en las propiedades del compuesto formado por los residuos de madera en forma de partículas y realizar su respectiva caracterización	El producto propuesto para utilizar la nanocelulosa fueron bloques de madera utilizados en la fabricación de tarimas tipo europea. Los bloques de madera compuesta fabricados con PVAc y UF y modificados con NCC al 1% con tres especies tropicales (*Vochysia ferruginea*, *Cordia alliodora* y *Gmelina arborea*), comúnmente usadas en la fabricación de tarimas en Costa Rica, mejora el comportamiento en la flexión estática de la tarima tipo europea, específicamente en los valores de carga máxima y deflexión. Este resultado, junto con las pruebas realizadas a los bloques de madera compuesta, indica que al sustituir el bloque de madera sólida por un bloque compuesto y agregar a los adhesivos NCC al 1% es una opción viable y con un alto desempeño estructural de la tarima tipo europea.

CONCLUSIONES GENERALES

La adición de NCC al 1% mostró un aumento en la cohesión interna, en la prueba de extracción de clavos en los bloques de la madera de *Vochysia ferruginea*, *Cordia alliodora* y *Gmelina arborea* para fabricar tarimas tipo europea en los adhesivos PVAc y UF, mostrando así que la NCC mejora las propiedades de resistencia de los adhesivos utilizado en madera. No obstante, a pesar que la absorción de agua disminuye con la adición de NCC, esta no llega a los niveles de un bloque de madera sólida. Siendo este aspecto un factor de cuidado en el momento de fabricar tarimas con este tipo de bloques.

Los bloques de madera compuesta fabricados con PVAc y UF y modificados con NCC al 1% con las tres especies tropicales, comúnmente usada en la fabricación de tarimas en Costa Rica, mejora el comportamiento en la flexión estática de la tarima tipo europea, específicamente en los valores de carga máxima y deflexión. Este resultado, junto con las pruebas realizadas a los bloques compuestos, indica que el sustituir el bloque de madera sólida por un bloque compuesto y agregar a los adhesivos NCC al 1% es una opción viable y con un alto desempeño estructural de la tarima tipo europea.

Articulo 1: Micro- and nanofibrillated cellulose extracted from pineapple (*Ananas comosus*) stems and its application in polyvinyl acetate (PVAc) and urea-formaldehyde (UF) wood adhesives

Priscilla Rigg[1], Róger Moya[2*], José Vega-Baudrit[3], Gloria S. Oporto[4], Ricardo Starbird[5], Allen Puente-Urbina[6], Daniel Méndez[7], Luis Diego Potosme[8] and Marianelly Esquivel[9].

[1] Escuela de Ingeniería Forestal, Instituto Tecnológico de Costa Rica, Cartago, Costa Rica. Apartado 159-7050, Email: rigg2112@gmail.com, ORCID: 0000-0001-6150-4884
[2] Escuela de Ingeniería Forestal, Instituto Tecnológico de Costa Rica, Cartago, Costa Rica. Apartado 159-7050, Email: rmoya@itcr.ac.cr, ORCID: 0000-0002-6201-8383
[3] Laboratório Nacional Nanotecnologia (LANOTEC), Centro Nacional de Alta Tecnologia-CENAT, San Jose, Costa Rica. Email: jvegab@gmail.com, ORCID: 0000-0002-2002-1744
[4] School of Natural Resources, West Virginia University, Morgantown, WV 26506, USA, Email: gloria.oporto@mail.wvu.edu, ORCID: 0000-0001-7115-1154
[5]Centro de Investigación y de Servicios Químicos y Microbiológicos (CEQIATEC), Escuela de Química, Instituto Tecnológico de Costa Rica, Costa Rica. Apartado 159-7050, Email: rstarbird@itcr.ac.cr, ORCID: 0000-0002-0700-0594
[6]Centro de Investigación y de Servicios Químicos y Microbiológicos (CEQIATEC), Escuela de Química, Instituto Tecnológico de Costa Rica, Costa Rica. Apartado 159-7050, Email: apuente@itcr.ac.cr, ORCID: 0000-0001-5328-2142
[7]Laboratorio de Polímeros, Escuela de Química, Universidad Nacional de Costa Rica, Heredia. Costa Rica, Email: dmendezmasis23@gmail.com
[8]Laboratorio de Polímeros, Escuela de Química, Universidad Nacional de Costa Rica, Heredia. Costa Rica, Email: ludipogo@gmail.com
[9]Laboratorio de Polímeros, Escuela de Química, Universidad Nacional de Costa Rica, Heredia. Costa Rica, Email: marianelly.esquivel.alfaro@una.cr

ABSTRACT

Nanocellulose as micro- and nanofibrillated forms (MNFC) was extracted from pineapple stem by acid hydrolysis, then characterized and tested in two concentrations (0.5 and 1.0 w/w%) in polyvinyl acetate (PVAc) and Urea-formaldehyde (UF) adhesives. The modified adhesives were used to glue three tropical wood species (Vochysia ferruginea, Cordia alliodora and Gmelina arborea). MNFC and the adhesives were characterized by TGA, FT-IR, SEM, TEM, AFM, viscosity and bond strength resistance. The TGA of MNFC showed three decomposition reactions. The SEM analysis showed that the dimensions of microfibrillated celulose varied between 4 and 20 µm in diameter and approximately 200 µm in length. The TEM and AFM images showed that the dimensions of nanofibrillated cellulose varied between 2 and 30 nm in diameter and 200 nm in length. Adding 0.5 w/w% MNFC to PVAc adhesive, and 1 w/w% MNFC to UF adhesive increased their thermal stability. The FTIR showed the characteristic signals of the hydrogen bonds (O-H groups) appeared at 3334 and 1635 cm^{-1}. TEM images showed good dispersion of MNFC in the adhesives. Viscosity diminished in both adhesives modified with MNFC, however this diminution did not affect the adhesion properties in the wood species tested. MNFC added to PVAc and

UF adhesives improved shear strength of the glue line (SS) in the three tropical species tested. The highest SS increase was obtained when adding 0.5 w/w% MNFC to PVAc in V. ferruginea, and 1 w/w% MNFC concentration in the case of C. alliodora and G. arborea. In C. alliodora and G. arborea, the highest SS was obtained with 1% MNFC concentration in UF.

KEYS WORDS

Key words: micro-nanocelullose, wood adhesives, tropical species, pineapple stem

INTRODUCTION

Cellulose is the most abundant organic compound in the Earth (Li et al, 2009). It is a biopolymer with formula $[C_6H_{10}O_5]_n$ (Li et al, 2009) and its repeating unit is cellobiose (Lavoine et al., 2012, French, 2017). It is one of the few naturally formed polymers as it is synthesized by all plants together with other also important components such as lignin, hemicellulose and waxes (Morán et al., 2008). Cellulose is found in all plant parts, concentrating mainly in the stem (Lavoine et al, 2012; Morán et al, 2008), whose major function is to provide structure and support to the plant (Morán et al, 2008). Cellulose is a biosynthesized material in the form of microfibers with amorphous and crystalline domains, with O-H groups that allow hydrogen bonding between molecules (Lavoine et al, 2012, French, 2017). The amorphous zones present randomly oriented fibres, while the crystalline zones show better fibre organization that provides increased density, therefore higher strength (Li et al, 2009).

Because of its renewable nature and its physical and chemical characteristics, cellulose has gained relevance in material development in the last decades (Poletto et al., 2014). Cellulose dimensions —20 microns in diameter and 100-400 microns in length— allow extraction of microfibrillated cellulose and nanocrystalline cellulose (MNCC) from it (Morán et al, 2008). MNCC is extracted by means of chemical methods such as acid hydrolysis, which allows the rupture of amorphous zones within the fibres, leaving crystalline zones only. Amorphous domains within the cellulose present faster hydrolysis kinetics than crystalline zones, acting as division points within the fibres during hydrolysis, thus decreasing the length from micro to nano scale (Johar et al., 2012), with dimensions of 15-20 nm in diameter and lengths of 200-500 nm (Li et al, 2009).

The most important materials for MNCC extraction are annual cultures because of being abundant, biodegradable and seldom utilized (Dos Santos et al., 2013; Draman et al., 2016). Several authors have studied the MNCC extracted from corn, wheat, rice, coconut, soy (Maepa et al, 2015), and jute and pineapple leaves (Dos Santos et al, 2013; Draman et al, 2016). The firstly mentioned materials present high concentrations of cellulose compared to other raw materials such as wood (Poletto et al, 2014).

Because of the strength provided by its crystalline nature, low molecular weight and biodegradability (Liew et al, 2015), MNCC has been studied and utilized as reinforcement and filler of various polymers (Poletto et al, 2014). The wood industry has implemented the use of reinforcing and protecting materials in the adhesives to increase their mechanical properties (Chaabouni & Boufi, 2017; Moya et al., 2015a-2015b). Several studies have showed that adding cellulose in the form of MNCC to the two most important adhesives in the wood industry (UF and PVAc) improves their strength (Chaabouni y Boufi, 2017; Kwon et al., 2015).

Pineapple (*Ananas comosus*) is an annual culture that produces around 24.8 million tons per year (Darnaudery et al., 2016; Draman et al, 2016). However, this activity produces large amounts of residues in the form of leaves, stems, crowns and fruit peel that are not used, which is a drawback (Rattanapoltee & Kaewkannetra, 2014). This has led to the search for information regarding better use and improved performance of pineapple raw material (Draman et al, 2016).

Several studies have analysed nanoparticle application in the formulation of adhesives used with tropical species, finding promising results (Moya et al, 2015a; 2015b). However, no studies have been found so far relative to MNCC addition to wood adhesives for making products from tropical species. Therefore, the aim of this work was to characterize MNCC from pineapple stem by thermogravimetric analysis, infrared spectroscopy and microscopy [Scanning Electron Microscopy (SEM), Transmission Electron Microscopy (TEM) and Atomic Force Microscope (AFM)]. Our purpose was to determine the effect of adding three MNCC concentrations in two adhesives (polyvinyl acetate and urea-formaldehyde) commonly used in wood, by means of thermogravimetric analysis, infrared spectroscopy, electronic transmission microscopy, viscosity and shear strength of the glue line in *Vochysia ferruginea, Cordia alliodora* and *Gmelina arborea* in Costa Rica.

MATERIALS AND METHODS

Materials

The cellulose extracted from the pineapple stem was provided by the startup Reuti-piña (http://reuti-pinacr.com/) and the Laboratorio de Ciencia y Tecnología de Polímeros de la Universidad Nacional (POLIUNA).

Two adhesive types were tested. Firstly, water-based polyvinyl acetate (PVAc) of the brand Resistol M.R. 850, produced by Henkel Capital S.A. (http://www.resistol.com.mx/es.html). The technical description of this product indicates that the resin is PVAc dissolved in water with 54.5-55.0% solid contents and 1600-2000 cPs viscosity. The second adhesive was water-based Urea-formaldehyde (UF) of the brand Resina CR-560 U-F, manufactured by Química Centroamericana, Quibor, S.A. (http://www.agroquibor.com/). This second adhesive has 4 components: resin (51%), water (26%), wheat flour as binder (20%), and ammonium sulphate as catalyser (3%). The technical description indicates that pure resin contains 64-65% solid contents and 650-900 cPs viscosity. Solids content of the complete

adhesive with the 4 components is 48%. This solids content was determined by means of an Ohaus MB45 thermal balance at 105° C, using three adhesive samples.

Three tropical plantation species in Costa Rica were used to evaluate the effect of MNCC in both types of adhesive: *Gmelina arborea* Roxb., *Vochysia ferruginea* Mart and *Cordia alliodora* Ruiz & Pav. These are commercial species commonly used to manufacture pallets in Costa Rica [Oficina Nacional Forestal (ONF), 2017].

Micro-nanocrystalline cellulose extraction

Figure 1 shows the process of extraction of MNCC from pineapple stem as described by Oun and Rhim (2016), with modified concentrations, equipment and reaction times. It was a two-part process. Firstly, the microfibrillated cellulose was extracted from pineapple stems, and secondly, the MNCC was extracted. A detailed description of both parts follows.

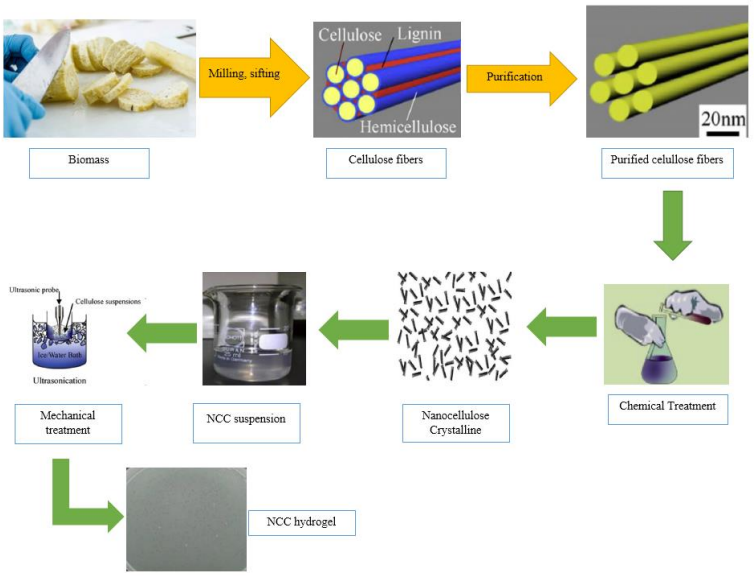

Figure 1. General process of micro-nanocrystalline cellulose hydrogel production from pineapple stem (Ng et al, 2015, Aranwit & Bang, 2014).

Microfibrillated cellulose: the pineapple stem was cut into 2 cm-long pieces and then dried at 80 °C until reaching 4% moisture content. Then, the pieces were ground to 300 µm size. A 2.5% sodium hydroxide (NaOH) solution was prepared and poured into the ground pineapple stem. The mixture was then heated up to 100°C for 4h. Following, the material was washed with distilled water to achieve neutral pH and then bleached with 4% sodium hypochlorite (NaClO) during 2h. Next, the material was washed with distilled water again to obtain neutral pH. These processes were applied as described by Rambabu et al. (2016), modifying the solution concentration and reaction times. MNCC was obtained by chemical hydrolysis reaction using a 2.5 N concentration hydrochloric acid (HCl) solution, using a reflux system at a temperature of 90 °C for a period of 30 min and subsequent filtration and neutralization with distilled

water, according to the process described by Gaspar et al. (2014) with modifications in concentrations and times.

Micro-nanocrystalline cellulose extraction: the MNCC was treated with 64% sulfuric acid (H_2SO_4) at ambient temperature during 1h. A pH between 3 and 5 was obtained by dialysis. Then the MNCC hydrogel (0.033g ml^{-1}, m v^{-1}) was obtained mechanically using ultrasound (Amplitude 70, 10min time).

Preparation of adhesives with MNCC

Two types of wood adhesives were utilized, PVAc and UF. The MNCC was added in three concentrations: 0% (control), 0.5% and 1.0% (weight $weight^{-1}$), added according to the percentage of solids in each adhesive (55% in PVAc and 48% in UF). The denominations for these concentrations are detailed in Table 1.

Table 1. Different nanocrystalline cellulose concentrations (w/w %) utilized in polyvinyl acetate and urea-formaldehyde adhesives for wood.

	Adhesive type					
	Polyvinyl acetate (PVAc)			Urea-formaldehyde (UF)		
Nanocrystalline cellulose concentration (w/w %)	0.0	0.5	1.0	0.0	0.5	1.0
Abbreviations	MNCC0-PVAc	MNCC5-PVAc	MNCC1-PVAc	MNCC0-UF	MNCC5-UF	MNCC1-UF

We prepared the MNCC-adhesive mixture as follows. For PVAc, 150 grams were placed into a pot and stirred with a 45°-inclined blade agitator at 1600 rpm; then, a proportion of MNCC gel (approximately 13.75 ml for 0.5% concentration and 27.5 ml for 1.0% concentration) was slowly added into the adhesive and stirring continued for 10 minutes. As for UF, because of its 4 components (resin, water, wheat and ammonium sulphate as catalyser), 76.5 g of the resin was mixed with 12 ml and 24 ml for 0.5% and 1.0% MNCC concentrations, respectively, stirring during 5 minutes at 1600 rpm with the help of an inclined blade agitator. The remaining components were then added (27.15 ml water, 30 g flour and 4.5 ml catalyser) and stirring continued for 5 more minutes.

Characterization of the micro-nanocrystalline cellulose and adhesives

The MNCC was characterized by AFM, SEM and TEM for distribution and its sizes, while the various types of adhesives were characterized by TGA, IR, viscosity and the bond strength resistance.

Thermogravimetric analysis (TGA)

Thermal stability of the MNCC and the two types of adhesives in the three MNCC concentrations were analysed in triplicate with a 6-7 mg sample in this analysis. TGA 5000 of the brand Instrument NBr was used. A heating rate of 25 °C/min from ambient temperature up to 1000° C was applied in the TGA test, under nitrogen atmosphere with a flow of 90 ml min^{-1}. To analyse the information obtained, the curves of the remaining mass versus temperature (degradation curves) were developed, then the reactions were identified with the help of the derivative of weight (DTG) with respect temperature. The reactions during

the decomposition of each adhesive were identified in these two curves. The degradation curves and DTG were obtained by means of the TA Instruments Universal Analysis 2000, observing the following parameters in each reaction: initial degradation temperature (T_i), maximum degradation temperature (T_{max}), final degradation temperature (T_f), percentage of remaining mass at initial temperature (MR_i), remaining mass at maximum temperature (MR_{max}) and remaining mass at final temperature (MR_f).

Following, the thermal stability, activation energy (E) and entropy factor (A) were determined. The data were modelled with the Gaussiana curve (Equation 1) and the MagicPlot software to determine the variables of the model (Equation 2). Next, considering a normal distribution and that the constant "c" in Equation 1 is equal to the standard deviation (σ), the values of the initial, maximum and final temperatures correspond to $x_0 \pm 3c$, considering 99,7% of the population; thus, the values of x_0 and dx were substituted by the values given by the software. Therefore, Equations 3 and 4 cleared "c".

$$f(x) = ae^{\frac{-(x-b)^2}{2c^2}} \quad (1)$$

$$f(x) = ae^{\frac{-\ln(2)(x-x_0)^2}{dx^2}} \quad (2)$$

$$-\frac{1}{2c^2} = -\frac{\ln(2)}{dx^2} \quad (3)$$

$$c = \frac{dx}{\sqrt{2\ln(2)}} \quad (4)$$

Where a, b and c are real constants (c > 0), *f(x)* is the derivative of weight and x is the temperature in °C.

Kinetics in each reaction was calculated by means of the Doyle model (Equation 5) (Saddawi et al., 2009). The model was applied to determine the following parameters for each reaction in both adhesives: E, which is the energy needed for each reaction to occur, and A, which is specific for each reaction and is interpreted as the number of collisions between the molecules that occur during the reaction (Kotz et al., 2009).

$$\ln[-\ln(1-\alpha)] = \ln\left(\frac{AE}{BR}\right) - 1.0518\frac{E}{RT} - 5.33 \quad (5)$$

Where α: degraded mass, A: entropy factor, E: activation energy, T: temperature.

Fourier-transform infrared (FTIR) spectra

FT-IR was evaluated for MNCC and both adhesives in the three MNCC concentrations in dry condition. A 50 ml MNCC gel sample was taken and placed into a crucible in the oven during 24 h at 60 ºC. The complete dry sample was used for the analysis. After mixing the adhesives with the MNCC, 2 g of the mixture were placed on glass and were left to dry during 72 h, then the material was pulverized with a mortar and a sample (around 2 g) of the dry material was taken. The IR spectrum was registered using a Nicolet 6700 Thermoscientificen in ATR reflactant mode (equipped with a diamond crystal) within a range of 600-4000 cm^{-1}, a resolution of 4 cm^{-1} and taking 16 scans. The spectrum of each one of the conditions was analysed using the OMNIC program and the signals for each sample were identified.

Observations in TEM, AFM and SEM

As for TEM observations, a MNCC sample in pure condition was taken and diluted at 1.9% v v^{-1} in distilled water. The sample was put into a vial in an ultrasonic bath for 15 min at a frequency of 40 kHz. When the solution was ready, a 5 drop sample was taken and placed on the grid (covered with formvar) with the help of a syringe, and left for 5 minutes for the grid to retain the sample. Then, the grid was left to dry for 2 days and the dispersion and size of the MNCC were observed in the TEM (Jeol JEM 2100) at an acceleration of 200 kV. A drop of the mixture of each adhesive was placed on paraffin paper on top of two slides to obtain a fine sheet of the material in order to observe MNCC dispersion in the adhesives through the TEM.

As for AFM observations, 1 ml of the 19% MNCC solution was placed on a mica surface with the aid of a dropper and left to dry for 2 days. The surface topography of the MNCC sample was observed by means of an Asylum Research operated in the air-tap mode. Silicon probes were used (model Tap150Al-G, rear part of the overhang covered with Al) with resonance frequency of 150 kHz and 5 N m^{-1} force constant.

With regard to SEM observations, the size of microfibers was measured; one drop of the 1.9% v v^{-1} solution was placed on a glass slide with carbon tape and left to dry for 3 days; then the dry sample was coated with gold-palladium before analysis. A SEM of the brand Jeol JSM-5900 LV at 20kV acceleration voltage was used.

Viscosity of the adhesives

Viscosity was evaluated for both adhesives in the three MNCC concentrations. Measurements were performed at 20° C using a Discovery HR-3 hybrid rheometer with parallel disc geometry of 25 mm diameter, 500 µm between discs, applying shear rates between 0-200 s^{-1}.

Bond strength resistance

The bond strength resistance of the two types of resin with added MNCC in three concentrations was evaluated based on the shear strength of the glue line test (SS), according to ASTM D-905-98

(ASTM, 2013). After preparing the two types of adhesives with MNCC, the woods of three tropical species (*Gmelina arborea*, *Vochysia ferruginea* and *Cordia alliodora*) were prepared and glued. Ninety shear tests were carried out in total (30 samples per concentration x 3 concentrations) per species. The wood was stabilized at a condition of 12% moisture content for one week. The adhesive was applied in accordance with the manufacturer's specifications, which recommend an amount of 100 gm^{-2} for both adhesives. After applying glue to the wood surface, the samples were pressed in a hydraulic machine at 0.20 Nmm^{-2} for 24 hours. Before pressurizing, glued samples were conditioned to 20 °C and 60% relative humidity for two weeks. Next, 30 samples were extracted from the glued samples and tested for each set of formulation per species. The SS was measured under dry ambient air conditions. A Tinus Olsen hydraulic test machine with 50 kN capacity was used for load application and the data were acquired by means of a computer.

Analysis of the information

Compliance of the variables determined with the assumptions of the normal distribution, variance homogeneity and the presence of outliers, was verified. Subsequently, a variance analysis was performed to verify the effect of the MNCC adhesion (three levels: 0.0%, 0.5% and 1.0%) on the values of E, A, the different temperatures and remaining masses in the various reactions of the decomposition kinetics, in addition to the bond strength resistance. The Tukey test at 99% confidence level was applied to determine the statistical difference between averages.

RESULTS AND DISCUSSION

Thermal stability analysis (TGA)

TGA analyses for pure MNCC and for the adhesives with three concentrations of MNCC (0.0, 0.5% and 1.0%) are shown in Figures 2a and 2b. Two inflections appear in pure MNCC, at 200 °C and at 350 °C (Figures 2a and 2b). These temperatures agree with studies by Kargarzadeh et al (2012), where temperatures of 230 °C and 350 °C are reported, and of Kumar et al. (2014), who report values of 220°C and 330°C for MNCC extracted by acid hydrolysis from sugarcane and kenaf, respectively.

It was possible to develop 3 fitting curves for the MNCC (Table 2), each one corresponding to 3 reactions. Reaction 1 occurred between 169 °C and 252 °C, reaction 2 occurred between 199 °C and 282 °C, and reaction 3 occurred along the whole decomposition process, from 37 °C to 693 °C. Decomposition T_i of MNCC from pineapple stem in this study was lower than the one reported by other studies. For example, Dos Santos et al (2013) reported T_i of 225 °C in MNCC obtained from pineapple leaves by acid hydrolysis; Costa et al (2013) and Hammiche et al (2016) indicated cellulose degradation T_i at 210 ºC for MNCC extracted by steam pressure from pineapple leaves and by acid hydrolysis from alfa fibres in both studies. Decrease in MNCC thermal stability may be due to extensive particle surface since hydrolysis promotes shorter MNCC chains (Kargarzadeh et al, 2012; Kumar et al, 2014).

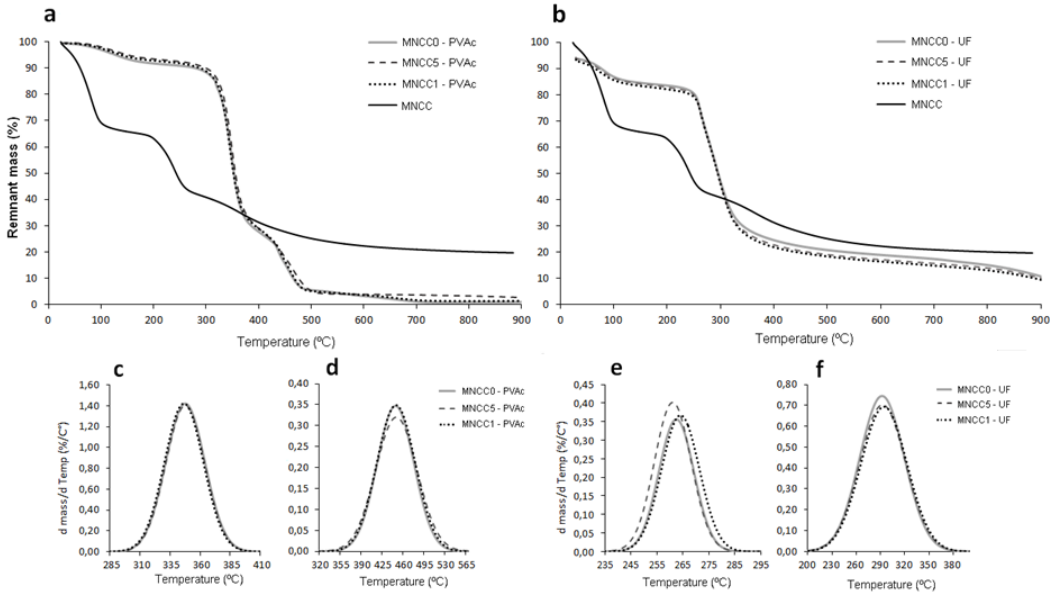

Figure. 2. TGA and DTG of different reaction curves of PVAc (a, c and d) and UF (b, e, f) wood adhesives, adding different concentrations of MNCC.

Figure 3 shows the curves of three reactions detected in pure MNCC. MNCC production by cellulose degradation involves processes of dehydration, depolymerisation, decomposition of glycoside bonds and carbonization (Kumar et al, 2014). On the other hand, MNCC produced by acid hydrolysis incorporates surface sulphate groups to the MNCC chains due to sulfuric acid of the hydrolysis (Chen et al., 2009). Degradation of the MNCC sulphate groups can be observed in the reactions in the TGA, at the maximum point of reaction 1 (at 210 °C) and in reaction 2 which started after T_{max} at 240.6 °C (Kargarzadeh et al, 2012, Kumar et al, 2014). Roman & Winter (2004) support these results when they analyse the MNCC extracted by acid hydrolysis from bacterial cellulose. These authors mention that initial MNCC decomposition corresponds to sulphate groups added to the amorphous zones of the MNCC during hydrolysis, producing a first peak in the DTG curve. They also mention that sulphate groups also adhere to the MNCC crystal chains, causing a second decomposition peak. These two reactions permit accessibility to cellulose nanocrystals and degradation, giving rise to a third process of decomposition corresponding to the whole range of temperatures from 100 °C to 700 °C, with decomposition T_{max} at 365.42 °C.

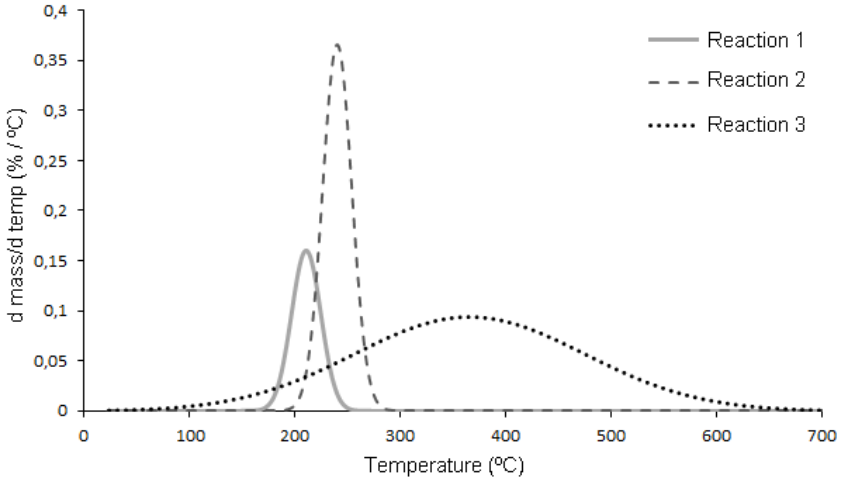

Figure 3. Fitting curves of the MNCC decomposition processes.

Complete MNCC decomposition in this study took place between 338 ºC and 350 ºC (Figure 3). Studies conducted by Abraham et al (2011), Costa et al (2013) and Draman et al. (2016) agree with these results. These authors extracted MNCC from pineapple leaves by means of the methods of acid hydrolysis and steam pressure, acid hydrolysis and an eco-friendly method of solution in eutectic solvent (choline chloride and urea).

The analysis of the TGA curves of the MNCC5-PVAc adhesive shows a slight increase in the decomposition temperature in relation to MNCC0-PVAc (Figure 2a). Moreover, if observed in detail, the thermal stability of both concentrations (Figure 2b) differ in UF adhesive, being higher in MNCC1-UF. This behaviour indicates increased thermal stability of the adhesive with MNCC, because degradation occurred at higher temperatures (Kaboorani et al, 2012) due to improvement of the MNCC fibres and the polymeric matrix.

In addition, TGA curves showed 2 inflexions of the PVAc adhesives with or without MNCC (Figure 2a), while only one inflexion was observed with UH adhesives with or without MNCC (Figure 2b). The first PVAc inflexions appeared around 346°C and the second inflexion at 448 °C, while in UF adhesive the inflexion occurred at 263 °C approximately. Greater mass loss occurred between 300 °C and 400 °C in both adhesives in all MNCC concentrations (Figure 2a-b).

DTG-temperature fitting curves are shown in Figures 2c and 2d. Figures 2e-f show the fitted two curves corresponding to the inflexions found in the TGA for PVAc, while for UF adhesive (Figures 2e-f) two curves were fitted. The second decomposition curve appears starting at 209 ºC with a maximum peak close to 290 ºC.

In PVAc adhesives, reaction 1 occurred between 297 °C and 396°C (Figure 2c), which is attributed to formation of volatile components and loss of acetate groups (deacetylation) (Holland & Hay, 2002). Reaction 2 occurred between 342 °C and 553 °C (Figure 2d), and is attributed to decomposition

of the main structure of the residues of the polyene polymer that turn into carbon and hydrocarbons (Holland & Hay, 2002; Lee et al., 2014).

Reaction 1 in the UF adhesive (Figure 2e-f), occurred between 239 °C and 285°C, and it refers to the degradation of the polymer because of the partition of the polymeric chains and formaldehyde emission from the dimethylene ether groups (Roumeli et al, 2012). Reaction 2 occurred within a higher range of temperatures, between 207 °C and 380 °C (Figure 2f), and is attributable to mass loss during fragmentation of the polymer residues (Jiang et al., 2010) in which methylene, methylol, dimethyl ethers, methylene glycols (formaldehyde) and components with carbonyl groups, among others, are freed (Moya et al., 2015b).

Relative to MNCC effect on the temperatures of reaction, a slight increase in T_{max} of the MNCC5-PVAc adhesive was observed for PVAc adhesive, as in MNCC1-UF (Figures 2c-f) in both reactions. This is congruent with reports from Kaboorani et al (2012), who added MNCC to PVAc adhesive to determine its mechanical and thermal effect in the adhesive. Increase in reaction T_{max} when adding MNCC to the adhesive was determined.

An important aspect to highlight in the curves of the adhesives and the pure MNCC curves is that the decomposition T_{max} of the two main reactions of pure MNCC occurred before the reactions of the adhesives: T_{max} was 347 °C and 448 °C on average for reactions 1 and 2, respectively, in PVAc adhesive, and in the UF adhesive, 262 °C and 292 °C for the reactions 1 and 2, respectively. This behaviour was also observed in a study where degradation at lower temperature of MNCC extracted by acid hydrolysis from commercial microcellulose with respect to polymer (polylactide and polyvinyl acetate) occurred. This is because pure MNCC appears in chains with broader surface area and nanoscale sizes that allow its rapid decomposition (Li et al., 2011), while adhesives present much stronger bonds between particles that make its decomposition more difficult (Jiang et al., 2010).

Table 2 shows temperatures and remaining mass in each reaction for the different MNCC concentrations in the two adhesives. There are small differences between temperatures (T_i, T_{max} and T_f) and remaining masses (MR_i, MR_{max} and MR_f) of reaction 1 in PVAc adhesive with the different MNCC concentrations. MNCC addition to the adhesive had a positive effect as an increase in T_i and T_{max} occurred in reaction 1 of MNCC5-PVAcv, whereas the opposite effect occurred with MNCC1-PVAc adhesive, for the three temperatures (T_i, T_{max} and T_f) diminished. Reaction 2 in MNCC0-PVAc and MNCC1-PVAc presented similar temperatures and remaining masses, and MNCC5-PVAc showed higher T_{max} and T_f, and greater MRi compared to the other concentrations. Similarly, MR_{max} showed no variations in reaction 2.

T_i and T_f in reaction 1 of UF adhesive exhibit small variations in the three concentrations (Table 2). T_{max} increased in MNCC1-UF, whereas in MR_i, MR_{max} and MR_f it tended to diminish as MNCC increased. Similar T_i were observed in reaction 2, whereas T_{max} and T_f tended to increase proportionally to MNCC percentage, and were higher in MNCC1-UF. Conversely, the remaining masses of the three decomposition points tended to decrease the higher the MNCC. Ash content was lower with 1% MNCC in both adhesives. In both adhesives the increase in temperatures and diminution of the remaining mass

when adding the MNCC was due to disordered network or particle agglomeration containing a crystalline structure formed by the MNCC that restricts mobilization of the material and slows down its decomposition (Chaabouni & Boufi, 2017, Lee et al, 2014).

Table 2. Temperature and remaining mass for different reactions for decomposition of PVAc and UF wood adhesive, adding different concentrations of MNCC.

Reaction	Parameter	MNCC Pure	MNCC concentration in PVAC			MNCC concentration in UF		
			0.0	0.5	1.0	0.0	0.5	1.0
Reaction 1	T_i (°C)	169.0	298.8	299.2	297.8	242.3	240.0	242.3
	MR_i (%)	65.2	90.5	89.5	90.1	81.8	80.8	77.4
	T_{max} (°C)	210.8	347.6	347.7	346.2	262.5	261.1	264.1
	MR_{max} (%)	61.1	60.4	59.9	60.5	73.6	72.6	68.9
	T_f (°C)	252.5	396.4	396.2	394.6	282.7	282.1	286.0
	MR_f (%)	46.3	29.5	29.1	29,7	58.9	57.9	53.6
Reaction 2	T_i (°C)	199.1	355.6	345.6	352.8	209.3	207.9	209.1
	MR_i (%)	63.3	52.2	62.4	52.8	83.6	82.2	79.0
	T_{max} (°C)	240.6	448.0	449.3	448.8	291.9	292.7	294.6
	MR_{max} (%)	50.9	17.7	17.5	17.4	52.1	50.6	47.7
	T_f (°C)	282.1	540.3	553.0	544.8	374.5	377.5	380.0
	MR_f (%)	42.0	4.8	4.0	3,91	25.2	24.6	21.9
Reaction 3	T_i (°C)	37.2	-	-	-	-	-	-
	MR_i (%)	96.9	-	-	-	-	-	-
	T_{max} (°C)	365.4	-	-	-	-	-	-
	MR_{max} (%)	34.8	-	-	-	-	-	-
	T_f (°C)	693.6	-	-	-	-	-	-
	MR_f (%)	21.0	-	-	-	-	-	-
Ash content		19.65	1.91	1.46	0.95	4.86	6.15	3.76

Table 3 shows the parameters A and E that determine MNCC combustion in both adhesives in the three MNCC concentrations. These values demonstrate dependence of reactions on calorific energy and are measured by temperature, therefore this parameter helps measure the reinforcement effect of MNCC on adhesives. Reaction 2 is the most energetic in pure MNCC as it presents higher E and A values. Contrariwise, reaction 3 presents the lowest values, therefore it is less energetic and less stable (Liew et al, 2015). The energy reaction 1 needs for decomposition to occur increased in MNCC1-PVAc adhesive, however, E value oscillated between 211 and 212 kJ $mol^{-}1$. On the other hand, in reaction 2 MNCC5-

PVAc exhibited the smallest value, while MNCC0-PVAc adhesive needed higher amount of energy to carry out decomposition. Kinetics evaluation of the UF adhesive showed that E in reactions 1 and 2 was lower than in MNCC1-UF. In contrast, MNCC5-UF presented higher E value (Table 3).

Adhesive	Reaction	MNCC (%)	Activation energy (kJ mol^{-1})	Entropy Factor (K_0 in s^{-1})	Correlation coefficient (R^2)
PVAc	1	0.0	211.45	2.87 x10 ^{17}	0.95
		0.5	212.59	1.21 x10 ^{17}	0.95
		1.0	212.67	2.01 x10^{17}	0.95
	2	0.0	90.10	1.30 x 10^{8}	0.93
		0.5	70.49	6.02 x 10^{4}	0.90
		1.0	83.90	3.52 x 10^{6}	0.93
UF	1	0.0	336.91	7.43 x 10^{35}	0.94
		0.5	345.64	5.77 x 10^{38}	0.94
		1.0	323.27	5.06 x 10^{34}	0.94
	2	0.0	118.71	1,10 x 10^{10}	0.94
		0.5	117.03	8,75 x 10^{9}	0.94
		1.0	115.42	5,22 x 10^{9}	0.94
	Reaction				
Pure MNCC	1		24.36	4.53 x 10^{2}	0.78
	2		130.42	4.00 x 10^{12}	0.93
	3		15.20	2.14 x 10^{1}	0.91

E is the energy necessary for reactants to interact and cause the reaction (Laidler, 1984), therefore it is also an indicator of the stability of the material (Liew et al, 2015). MNCC1-PVAc and MNCC5-UF adhesives presented better stability in reaction 1. The increase of stability in adhesives produced by the MNCC is due to the rigid network between the fibres resulting from hydrogen bonds of MNCC, increasing the resistance of the polymer to degradation (Boufi et al., 2014).

On the other hand, A is the frequency of the collisions between the particles during the reaction (Laidler, 1984), therefore it is an indicator of the speed of material decomposition (Rowe et al., 2016). A exhibits similar values in reaction 1 of PVAc adhesive in the three MNCC concentrations, while in reaction 2, MNCC5-PVAc showed the lowest value and MNCC0-PVAc presented better dynamics during the reaction. In adhesive MNCC1-UF, A exhibits the lowest value, while MNCC5-UF shows the highest value

of A for reaction 1. No differences were observed between the three concentrations in reaction 2 of adhesive UF. There was a tendency towards higher E and A (Table 3). A affects the rate of the reaction, increasing the frequency of the collisions and triggering the process of degradation (Hashemi et al, 2016). This effect was observed in E in reaction 1, increasing with MNCC1-PVAc and MNCC5-UF.

Table 3. Values of entropy factor, energy activation, function of decomposition degree and correlation coefficient of decomposition kinetics of PVAc and UF wood adhesives adding different concentrations of MNCC.MNCC.

Fourier-transform infrared (FTIR) spectra

Figures 4 show the FTIR spectrum of the MNCC and the PVAc and UF adhesives with added MNCC. For MNCC (Figure 4a-d) the characteristic signals of the hydrogen bonds (O-H groups) appeared at 3334 and 1635 cm^{-1}. These signals are produced by stretching and flexing of the bonds between the water particles inside the sample and the cellulose bonds. The signal at 2914 cm^{-1} corresponds to stretching of C-H of the cellulose (Johar et al, 2012; Liew et al, 2015), while sulphate groups added during the process of acid hydrolysis may be detected at signals close to 1350 cm^{-1}. In addition, the signals characteristic of the cellulose occurred at signal 1053 cm^{-1} corresponding to the bond C-O-C of the structure of the pyranose ring (Morán et al, 2008) and 896 cm^{-1} with groups C-H coming from the vibration of the glycosidic bonds among the glucose units (Chen et al, 2011; Draman et al, 2016). Likewise, these signals (1053 and 896 cm-1) are reported to denote the amorphous cellulose region (Poletto et al, 2014). The signal at 1428 cm^{-1} corresponded to the crystalline zone of the MNCC (Poletto et al, 2014), showing the two domains (amorphous and crystalline) within the MNCC.

In the PVAc adhesive (Figure 4b), the vibrations observed at 1725, 1377 and 1245-1275 cm^{-1} are related to the carbonyl group, methylene and to ester stretching, respectively (Mansoori et al., 2011). The signals at 1225 cm^{-1} and 1015 cm^{-1} are used to identify the presence of PVAc (Mansoori et al., 2011). On the other hand, peaks at 1660 cm^{-1} and 1090 cm^{-1} occurred due to stretching of the hydrogen bonds because of the presence of MNCC in the matrix (Johar et al, 2012). These signals were observed with more intensity in the adhesive with MNCC1-PVAc (Figure 4d). The signal at 1430 cm^{-1} indicates the presence of the $C\text{-}H_3$ group (Pal & Gautam, 2013).

Figures 4f-h show the spectrum of the UF adhesive at the signal 1000 cm^{-1} of the $N\text{-}H_3$ group. The peak at 760 cm^{-1} corresponded to N-H group and the signals 1145 and 1375cm^{-1} to the groups C-O ether and C-N, respectively (Jiang et al., 2010). In addition, between 1650–1550 cm^{-1}, characteristic resin functional groups were detected, such as amide and C=O (Zorba et al., 2008). The evidence of the presence of MNCC in the UF adhesive is the increase in the signal at 2935 cm^{-1}, produced by the flexure of the C-H cellulose bond (Li et al, 2011). When MNCC was added, the signal at 3300 cm^{-1} of the O-H group increased in both adhesives, indicating increased hydrogen bonds added by the MNCC (Hammiche et al., 2016).

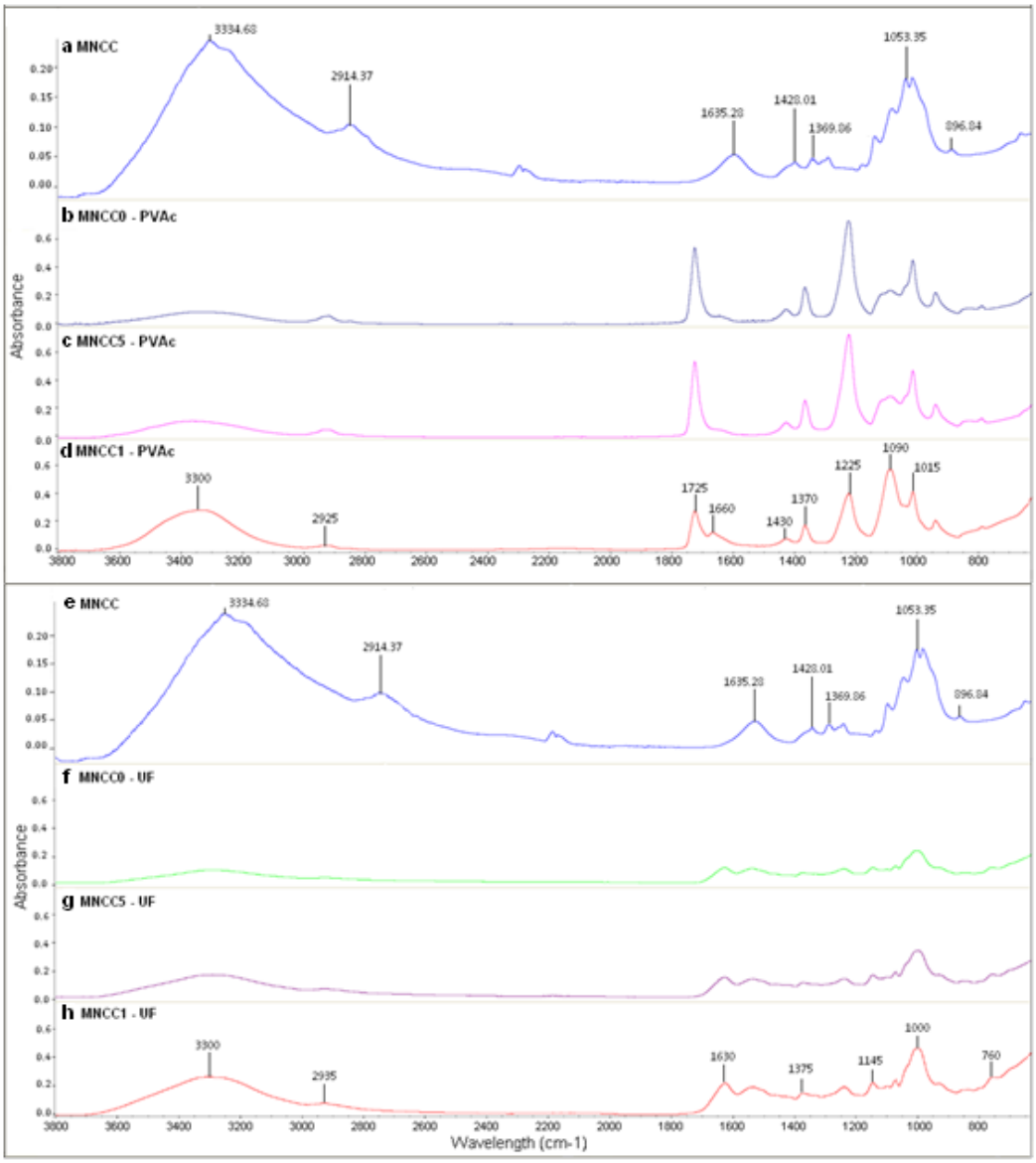

Figure 4. Fourier-transform infrared (FTIR) spectra of pure MNCC and adhesives modified with MNCC at different concentrations (a) PVAc wood adhesive and (b) UF wood adhesive.

Analysis of microscopy images

Microscopy images revealed the existing variation in the fibre dimensions and the micro-nanoscopic nature of the MNCC. The SEM analysis showed fibres of micrometric sizes over 200 µm in length and between 4 and 20 µm in diameter (Figure 5a). Moreover, the TEM image reflected a fibre network around 30 nm in diameter and more than 200 nm long, in addition to MNCC particles with similar diameters (Figure 5b), which was confirmed in the AFM image where the particle and fibre surface could be observed. The high points correspond to particles between 2-4 nm, while the fibres stand out with similar heights (Figure 6c-d). Acid hydrolysis processes allow to obtain fibres with diameters between 5-60 nm

and lengths between 200-300 nm, therefore the process applied to obtain MNCC from the pineapple stem fibre achieved fibre reduction. The MNCC dimensions obtained are congruent with Abraham et al (2011) and Dos Santos et al (2013) who extracted and evaluated MNCC from pineapple leaves by acid hydrolysis, achieving dimensions between 5-50 nm in diameter and 190-250 nm in length. These results agree with those of other studies applied to different raw materials and extraction methods, such as Cherian et al (2010) evaluating MNCC extracted from pineapple leaves by the method of steam explosion. These authors measured MNCC with diameters between 5-60 nm and lengths between 200-300 nm. Johar et al (2012), meanwhile, extracted MNCC from rice by acid hydrolysis, reporting diameters between 10-15 nm and lengths between 50-100 nm, and Li et al (2009) obtained MNCC between 25-30 nm in diameter and 400-500 nm in length from branches and bark of white mulberry (*Morus alba* L.) by acid hydrolysis. The results in this study are congruent with the previous values, as MNCC dimensions obtained are within the mentioned ranges.

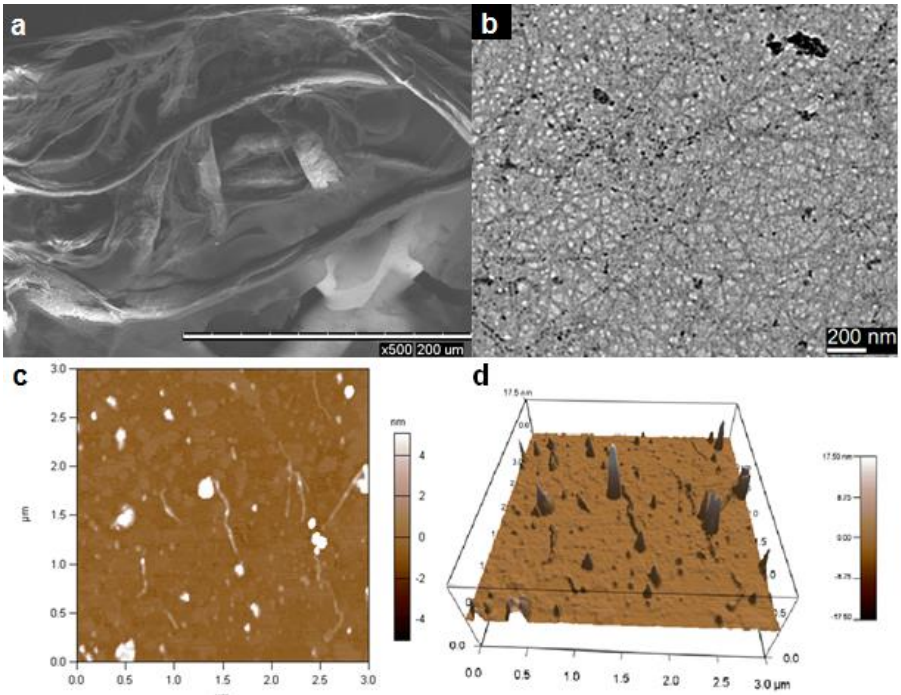

Figure 5**.** (a) Scanning Electron Microscopy-SEM, (b) Transmission Electron Microscopy (TEM) images and (c-d) Atomic force microscope-AFM spectra of MNCC.

MNCC dispersion will always be a determinant factor in material reinforcement as nanocellulose will tend to agglomerate because of its hydrophilic nature (Kargarzadeh et al, 2017). Adequate MNCC dispersion will improve the development of the properties of the adhesives and using water based material helps improve nanoparticle dispersion (Lee et al, 2014). TEM observations of MNCC showed adequate distribution. Figure 6 presents MNCC particle dispersion within the polymeric matrix of the UF adhesive. The matrix is completely even (Figure 6a). TEM image shows that the adhesive MNCC5-UF presents particles of 200 nm approximately (Figure 6b), while MNCC1-UF shows more varied particles which are dispersed throughout the material, forming agglomerations bigger than 1 µm (Figure 6c).

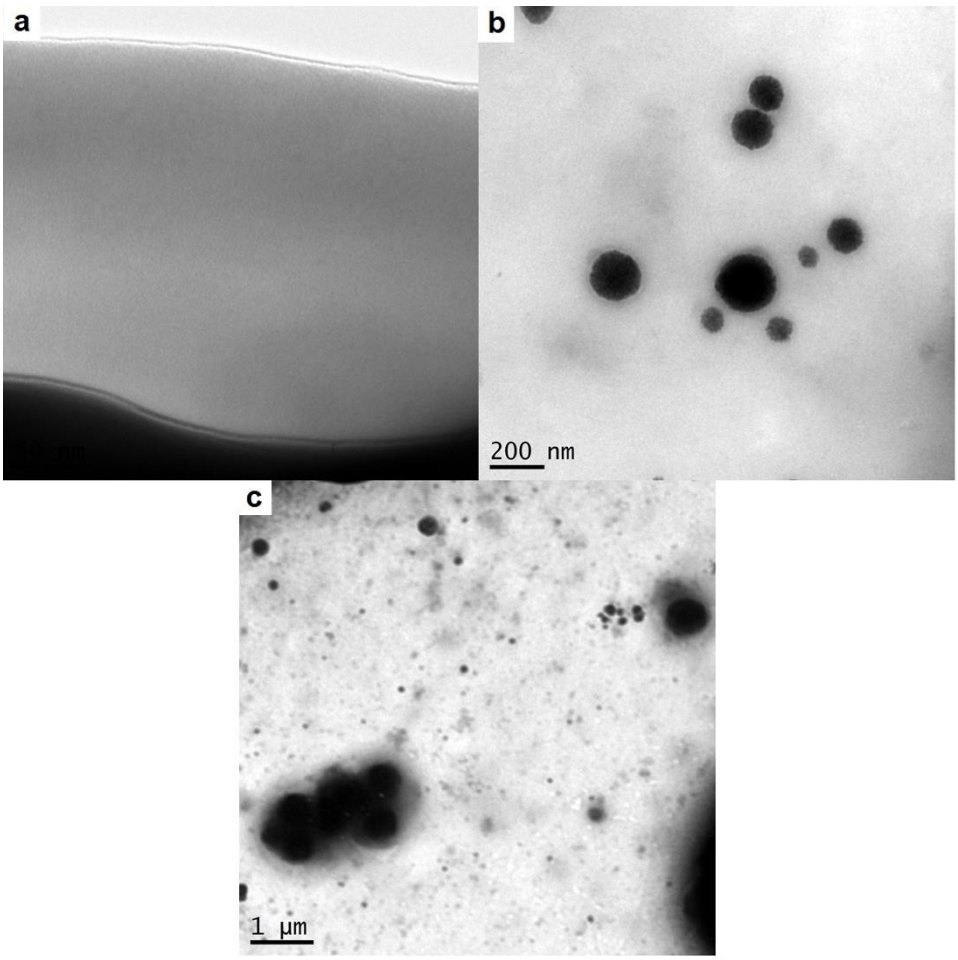

Figure 6. Transmission Electron Microscopy (TEM) images of UF wood adhesive with different concentrations of MNCC.

Viscosity

Figure 7 shows MNCC effect on the viscosity of the adhesives. As for MNCC concentration in PVAc (Figure 7a), the viscosity diminished with increasing MNCC concentration, varying between 40 and 15 Pa s at the starting point. This diminution is appropriate as higher concentrations of MNCC create paths for humidity, allowing moisture absorption (Gong et al., 2011). Adhesives with MNCC concentrations of 0.5% and 1% showed little variation because the most noticeable changes (increase) in viscosity in PVAc occurred at concentrations above 1%. This is because the joints formed between MNCC particles create a stronger network. Such behaviour was also observed in Chaabouni and Boufi (2017)'s work, where they added MNCC obtained by oxidation in the PVAc adhesive and tested it on *Eucalyptus globulus* wood. The same behaviour occurred in the UF adhesive, although the variation was smaller; viscosity decreased with increasing MNCC concentration (Figure 7b). The change in the rheological behaviour of the adhesive with the addition of MNCC comes from addition of water to the matrix, since the MNCC gel is made up of 97% water. Likewise, the shear force in the viscosity test broke

the polymer network, releasing trapped water (Chaabouni & Boufi, 2017) and thus decreasing the viscosity.

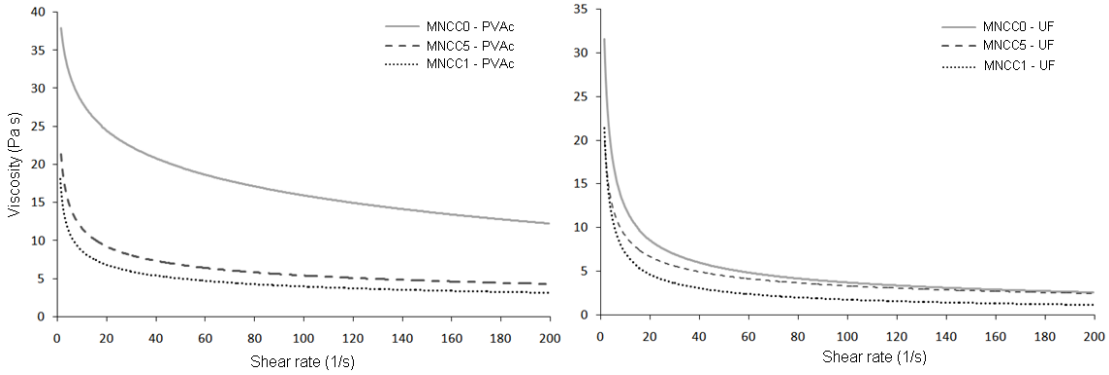

Figure 7. Viscosity values of PVAc and UF wood adhesives, adding different concentrations (wt.%) of MNCC (0%, 0.5%, 1%).5%, 1%).

Bond strength resistance

The results in the shear test show an increase in the SS with the addition of MNCC, both for the PVAc adhesive and for the UF adhesive, in all the species (Figure 8). An increase of SS in MNCC5-PVAc was observed in *V. ferruginea* with the adhesive PVAc, statistical differences occurring with MNCC0-PVAc, while for *C. alliodora* and *G. arborea* an increase of SS showed in MNCC1-PVAc (Figure 1a). The reinforcement of the UF adhesive with 1% MNCC (Figure 1b) in the three species increased the mechanical resistance of SS, despite the statistical differences between MNCC0-UF and the two concentrations of MNCC that occurred in *C. alliodora* and *G. arborea*.

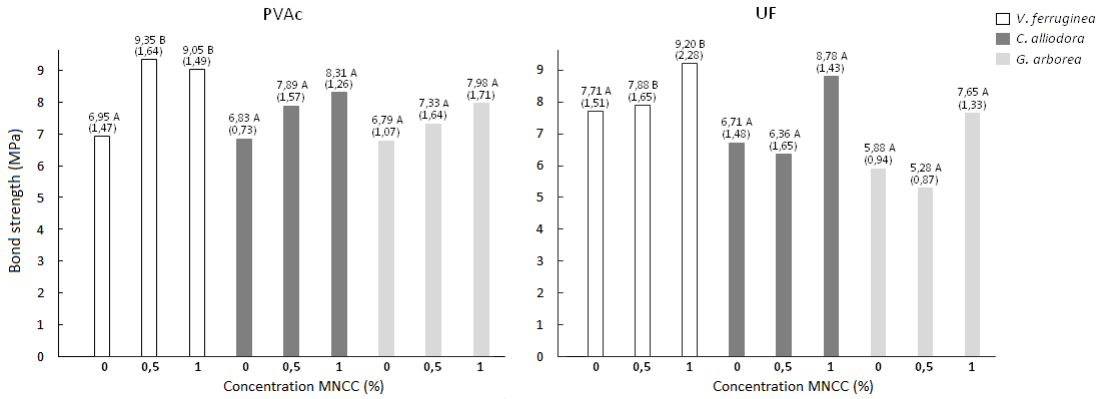

Figure 8. Resistance of shear strength in *V. ferruginea*, *C. alliodora* and *G. arborea* wood glued with PVAc and UF adhesive modified with MNCC in three concentrations.

Legend: The values between parenthesis represent standard deviation and average values identified with different letters are statistically different at α= 99%.

These results agree with Veigel et al. (2011), who mention that small amounts of MNCC can improve interactions within the material. Veigel et al (2011) and Zhang et al., (2011), adding 5% and 1.5%

MNCC concentration respectively, support our results confirming that there is an increase in the internal strength of the UF adhesive. Similar effect was observed in the PVAc adhesive, where the results of the present work agree with Chaabouni and Boufi (2017), Geng et al. (2016) and Pracella et al. (2012), where different MNCC concentrations were evaluated, finding an increase in adhesive shear strength with 10% MNCC in the first two works and 1% MNCC in the last work. On the other hand, Kwon et al. (2015) found that addition of 3% MNCC in the UF adhesive increased the SS.

These same authors (Kwon et al., 2015) mention that the increase of SS is because cellulose fibres in the glue line fill in the wood cavities together with the adhesive, allowing greater penetration, therefore much more strength is required to separate two pieces of wood. Likewise, the reinforcing effect of the wood-adhesive interface results from the formation of a network between the MNCC and the polymer chains of the adhesive (Grishkewich et al., 2017). Almeida et al. (2018) and Ramires and Dufresne (2012) explain that MNCC's broader contact area, high resistance to traction and rigidity, allows the formation of a network of crystals that interact with the adhesive, increasing its mechanical strength.

CONCLUSIONES

1. Nanocrystalline cellulose (MNCC) was obtained from pineapple stem by acid hydrolysis. The thermogravimetric analysis showed three decomposition curves of the MNCC. Decompositions 1 and 2 were due to degradation of sulphate groups, while cellulose decomposition showed in the last degradation curve. Analysis of microscopy showed that nanoscale cellulose fibres and particles can be obtained with dimensions ranging between 2-30 nm in diameter and 200-300 nm in length.
2. MNCC was adequately dispersed in polyvinyl acetate (PVAc) and urea formaldehyde (UF) adhesives according to TEM observations and FTIR signals where the presence of MNCC is evidenced. MNCC affected thermal stability of the adhesives, improving in MNCC5-PVAc, specifically, T_i, T_{max} in reaction 1 and T_{max} and T_f in reaction 2. Concerning UF, in MNCC1-UF T_{max} and T_f of reactions 1 and 2 were improved. Similarly, E and A increase in reaction 1 in MNCC5-UF adhesive. Viscosity was affected mainly by the addition of water contained in the MNCC gel, which was more evident in the PVAc adhesive, as its viscosity decreased.
3. MNCC added in PVAc and UF adhesives improved shear strength of the glue line (SS) in three tropical species tested. In *V. ferruginea* the highest increase was observed in MNCC5-PVAc, while for *C. alliodora* and *G. arborea* the increase in SS was observed in MNCC1-PVAc. In the UF adhesive, the highest resistance was obtained at 1% MNCC in *C. alliodora* and *G. arborea*.

ACKNOWLEDGEMENTS

The authors wish to thank the Vicerrectoría de Investigación y Extensión at the Instituto Tecnológico de Costa Rica for their assistance in conducting this study.

REFERENCES

Abraham, E., Deepa, B., Pothan, L. A., Jacob, M., Thomas, S., Cvelbar, U., & Anandjiwala, R. (2011). Extraction of nanocellulose fibrils from lignocellulosic fibres: a novel approach. *Carbohydrate Polymers*, *86*(4), 1468-1475. doi: 10.1016/j.carbpol.2011.06.034

Almeida, R. G., Mendes, L. M., Sanadi, A. R., de Sena Neto, A. R., Claro, P. I. C., Corrêa, A. C., & Marconcini, J. M. (2018). Urea Formaldehyde and Cellulose Nanocrystals Adhesive: Studies Applied to Sugarcane Bagasse Particleboards. *Journal of Polymers and the Environment*, 1-11. doi: 10.1007/s10924-018-1189-4

Aramwit, P., & Bang, N. (2014). The characteristics of bacterial nanocellulose gel releasing silk sericin for facial treatment. *BMC Biotechnology*, *14*(1), 104. doi: 10.1186/s12896-014-0104-x

ASTM. (2013). D905-08.Standard test method for strength properties of adhesive bonds in shear by compression loading. Annual Book of ASTM Standards 2013; VOL.11(06):5 p

Boufi, S., Kaddami, H., & Dufresne, A. (2014). Mechanical performance and transparency of nanocellulose reinforced polymer nanocomposites. *Macromolecular Materials and Engineering, 299*(5), 560-568. doi: 10.1002/mame.201300232

Chaabouni, O., & Boufi, S. (2017). Cellulose nanofibrils/polyvinyl acetate nanocomposite adhesives with improved mechanical properties. *Carbohydrate Polymers*, *156*, 64-70. doi: 10.1016/j.carbpol.2016.09.016

Chen, W., Yu, H., Liu, Y., Chen, P., Zhang, M., & Hai, Y. (2011). Individualization of cellulose nanofibers from wood using high-intensity ultrasonication combined with chemical pretreatments. *Carbohydrate Polymers*, *83*(4), 1804-1811. doi: 10.1016/j.carbpol.2010.10.040

Chen, Y., Liu, C., Chang, P. R., Cao, X., & Anderson, D. P. (2009). Bionanocomposites based on pea starch and cellulose nanowhiskers hydrolyzed from pea hull fibre: effect of hydrolysis time. *Carbohydrate Polymers, 76*(4), 607-615. doi: 10.1016/j.carbpol.2008.11.030

Cherian, B. M., Leão, A. L., de Souza, S. F., Thomas, S., Pothan, L. A., & Kottaisamy, M. (2010). Isolation of nanocellulose from pineapple leaf fibres by steam explosion. *Carbohydrate Polymers*, *81*(3), 720-725. doi: 10.1016/j.carbpol.2010.03.046

Costa, L. M. M., de Olyveira, G. M., Cherian, B. M., Leão, A. L., de Souza, S. F., & Ferreira, M. (2013). Bionanocomposites from electrospun PVA/pineapple nanofibers/*Stryphnodendron adstringens* bark extract for medical applications. *Industrial Crops and Products, 41*, 198-202. doi: 10.1016/j.indcrop.2012.04.025

Critchley, J. P., Knight, G. J., & Wright, W. W. (2013). *Heat-resistant polymers: technologically useful materials*. Springer Science& Business Media.

D'Amelia, R. P., Gentile, S., Nirode, W. F., & Huang, L. (2016). Quantitative Analysis of Copolymers and Blends of Polyvinyl Acetate (PVAc) Using Fourier Transform Infrared Spectroscopy (FTIR) and Elemental Analysis (EA). *World Journal of Chemical Education, 4*(2), 25-31. doi: 10.12691/wjce-4-2-1

Darnaudery, M., Fournier, P., & Lechaudel, M. (2016). Low-input pineapple crops with high quality fruit: Promising impacts of locally integrated and organic fertilisation compared to chemical fertilisers. *Experimental Agriculture*, 1-17. doi: 10.1017/S0014479716000284

de Morais Teixeira, E., Corrêa, A. C., Manzoli, A., de Lima Leite, F., de Oliveira, C. R., & Mattoso, L. H. C. (2010). Cellulose nanofibers from white and naturally colored cotton fibers. *Cellulose, 17*(3), 595-606. doi: 10.1007/s10570-010-9403-0

de Souza Lima, M. M., & Borsali, R. (2004). Rodlike cellulose microcrystals: structure, properties, and applications. *Macromolecular Rapid Communications*, *25*(7), 771-787. doi: 10.1002/marc.200300268

Dos Santos, R. M., Neto, W. P. F., Silvério, H. A., Martins, D. F., Dantas, N. O., & Pasquini, D. (2013). Cellulose nanocrystals from pineapple leaf, a new approach for the reuse of this agro-waste. *Industrial Crops and Products*, *50*, 707-714. doi: 10.1016/j.indcrop.2013.08.049

French, A. D. (2017). Glucose, not cellobiose, is the repeating unit of cellulose and why that is important. *Cellulose*, *24*(11), 4605-4609.

Draman, S. F. S., Daik, R., & Mohd, N. (2016). Eco-Friendly Extraction and Characterization of Cellulose from Lignocellulosic Fiber. *ARPN Journal of Engineering and Applied Sciences*, *11*(16), 9591-9595.

Gaspar, D., Fernandes, S. N., De Oliveira, A. G., Fernandes, J. G., Grey, P., Pontes, R. V., Pereira, L., Martins, R., Godinho, M. H., & Fortunato, E. (2014). Nanocrystalline cellulose applied simultaneously as the gate dielectric and the substrate in flexible field effect transistors. *Nanotechnology*, *25*(9).

Geng, S., Haque, M. M. U., & Oksman, K. (2016). Crosslinked poly (vinyl acetate)(PVAc) reinforced with cellulose nanocrystals (CNC): Structure and mechanical properties. *Composites Science and Technology*, *126*, 35-42. doi: 10.1016/j.compscitech.2016.02.013

Gong, G., Pyo, J., Mathew, A. P., & Oksman, K. (2011). Tensile behavior, morphology and viscoelastic analysis of cellulose nanofiber-reinforced (CNF) polyvinyl acetate (PVAc). *Composites Part A: Applied Science and Manufacturing, 42*(9), 1275-1282. doi: 10.1016/j.compositesa.2011.05.009

Grishkewich, N., Mohammed, N., Tang, J., & Tam, K. C. (2017). Recent advances in the application of cellulose nanocrystals. *Current Opinion in Colloid & Interface Science*, *29*, 32-45. doi: 10.1016/j.cocis.2017.01.005

Hammiche, D., Boukerrou, A., Djidjelli, H., Grohens, Y., Bendahou, A., & Seantier, B. (2016). Characterization of cellulose nanowhiskers extracted from alfa fiber and the effect of their dispersion methods on nanocomposite properties. *Journal of* Adhesion *Science and Technology, 30*(17), 1899-1912. doi: 10.1080/01694243.2016.1170586

Hashemi, S. M. B., Brewer, M. S., Safari, J., Nowroozi, M., Abadi Sherahi, M. H., Sadeghi, B., & Ghafoori, M. (2016). Antioxidant activity, reaction mechanisms, and kinetics of *Matricaria recutita* extract in commercial blended oil oxidation. *International Journal of Food Properties, 19*(2), 257-271. doi: 10.1080/10942912.2015.1020438

Holland, B. J., & Hay, J. N. (2002). The thermal degradation of poly (vinyl acetate) measured by thermal analysis–Fourier transform infrared spectroscopy. *Polymer*, *43*(8), 2207-2211. doi: 10.1016/S0032-3861(02)00038-1

Jiang, X., Li, C., Chi, Y., & Yan, J. (2010). TG-FTIR study on urea-formaldehyde resin residue during pyrolysis and combustion. *Journal of Hazardous Materials, 173*(1), 205-210. doi: 10.1016/j.jhazmat.2009.08.070

Johar, N., Ahmad, I., & Dufresne, A. (2012). Extraction, preparation and characterization of cellulose fibres and nanocrystals from rice husk. *Industrial Crops and Products*, *37*(1), 93-99. doi: 10.1016/j.indcrop.2011.12.016

Kaboorani, A., Riedl, B., Blanchet, P., Fellin, M., Hosseinaei, O., & Wang, S. (2012). Nanocrystalline cellulose (NCC): A renewable nano-material for polyvinyl acetate (PVA) adhesive. *European Polymer Journal*, *48*(11), 1829-1837. doi: 10.1016/j.eurpolymj.2012.08.008

Kargarzadeh, H., Ahmad, I., Abdullah, I., Dufresne, A., Zainudin, S. Y., & Sheltami, R. M. (2012). Effects of hydrolysis conditions on the morphology, crystallinity, and thermal stability of cellulose nanocrystals extracted from kenafbast fibers. *Cellulose*, *19*(3), 855-866. doi: 10.1007/s10570-012-9684-6

Kargarzadeh, H., Mariano, M., Huang, J., Lin, N., Ahmad, I., Dufresne, A., & Thomas, S. (2017). Recent developments on nanocellulose reinforced polymer nanocomposites: A review. *Polymer*. doi: 10.1016/j.polymer.2017.09.043

Kotz, J., Treichel, P.M., Townsend, J.R. (2009). *Chemistry & Chemical Reactivity*. Vol II. Thomson Books/Cole. Canadá.

Kumar, A., Negi, Y. S., Choudhary, V., & Bhardwaj, N. K. (2014).Characterization of cellulose nanocrystals produced by acid-hydrolysis from sugarcane bagasse as agro-waste. *Journal of Materials Physics and Chemistry, 2*(1), 1-8. doi: 10.12691/jmpc-2-1-1

Kwon, J. H., Lee, S. H., Ayrilmis, N., & Han, T. H. (2015). Tensile shear strength of wood bonded with urea–formaldehyde with different amounts of microfibrillated cellulose. *International Journal of Adhesion and Adhesives*, *60*, 88-91. doi: 10.1016/j.ijadhadh.2015.04.002

Laidler, K. J. (1984). The development of the Arrhenius equation. *J. Chem. Educ, 61*(6), 494.

Lavoine, N., Desloges, I., Dufresne, A., & Bras, J. (2012). Microfibrillated cellulose–Its barrier properties and applications in cellulosic materials: A review. *Carbohydrate Polymers*, *90*(2), 735-764. doi: 10.1016/j.carbpol.2012.05.026

Lee, K. Y., Aitomäki, Y., Berglund, L. A., Oksman, K., & Bismarck, A. (2014). On the use of nanocellulose as reinforcement in polymer matrix composites. *Composites Science and Technology*, *105*, 15-27. doi: 10.1016/j.compscitech.2014.08.032

Lee, S. Y., Mohan, D. J., Kang, I. A., Doh, G. H., Lee, S., & Han, S. O. (2009). Nanocellulose reinforced PVA composite films: effects of acid treatment and filler loading. *Fibers and Polymers, 10*(1), 77-82. doi: 10.1007/s12221-009-0077-x

Li, R., Fei, J., Cai, Y., Li, Y., Feng, J., & Yao, J. (2009). Cellulose whiskers extracted from mulberry: A novel biomass production. *Carbohydrate Polymers*, *76*(1), 94-99. doi: 10.1016/j.carbpol.2008.09.034

Li, W., Wang, R., & Liu, S. (2011). Nanocrystalline cellulose prepared from softwood kraft pulp via ultrasonic-assisted acid hydrolysis. *BioResources*, *6*(4), 4271-4281.

Liew, F. K., Hamdan, S., Rahman, M. R., Rusop, M., Lai, J. C. H., Hossen, M. F., & Rahman, M. M. (2015). Synthesis and characterization of cellulose from green bamboo by chemical treatment with mechanical process. *Journal of Chemistry*, *2015*. doi: 10.1155/2015/212158

Maepa, C. E., Jayaramudu, J., Okonkwo, J. O., Ray, S. S., Sadiku, E. R., & Ramontja, J. (2015). Extraction and characterization of natural cellulose fibers from maize tassel. *International Journal of Polymer Analysis and Characterization*, *20*(2), 99-109. doi: 10.1080/1023666X.2014.961118

Mansoori, Y., Akhtarparast, A., Reza Zamanloo, M., Imanzadeh, G., & Masooleh, T. M. (2011). Polymer–montmorillonite nanocomposites: Chemical grafting of polyvinyl acetate onto Cloisite 20A. *Polymer Composites, 32*(8), 1225-1234. doi: 10.1002/pc.21142

Morán, J. I., Álvarez, V. A., Cyras, V. P., & Vázquez, A. (2008). Extraction of cellulose and preparation of nanocellulose from sisal fibers. *Cellulose*, *15*(1), 149-159. doi: 10.1007/s10570-007-9145-9

Moya, R., Rodríguez-Zúñiga, A., & Vega-Baudrit, J. (2015a). Effects of adding multiwall carbon nanotubes on performance of polyvinyl acetate and urea-formaldehyde adhesives in tropical timber species. *Journal of Nanomaterials*, *16*(1), 290. doi: 10.1155/2015/895650

Moya, R., Rodríguez-Zúñiga, A., Vega-Baudrit, J., & Álvarez, V. (2015b). Effects of adding nano-clay (montmorillonite) on performance of polyvinyl acetate (PVAc) and urea-formaldehyde (UF) adhesives in *Carapa guianensis*, a tropical species. *International Journal of Adhesion and Adhesives*, *59*, 62-70. doi: 10.1016/j.ijadhadh.2015.02.004

Ng, H. M., Sin, L. T., Tee, T. T., Bee, S. T., Hui, D., Low, C. Y., & Rahmat, A. R. (2015). Extraction of cellulose nanocrystals from plant sources for application as reinforcing agent in polymers. *Composites Part B: Engineering, 75*, 176-200. doi: 10.1016/j.compositesb.2015.01.008

Oficina Nacional Forestal [ONF] (2017). Estadísticas 2016. Usos y Aportes de la Madera en Costa Rica.

Oun, A. A., & Rhim, J. W. (2016). Characterization of nanocelluloses isolated from Ushar (*Calotropis procera*) seed fiber: effect of isolation method. *Materials Letters*, *168*, 146-150. doi: 10.1016/j.matlet.2016.01.052

Pal, M. K., & Gautam, J. (2013). Effects of inorganic nanofillers on the thermal degradation and UV-absorbance properties of polyvinyl acetate. *Journal of Thermal Analysis and Calorimetry*, *111*(1), 689-701. doi: 10.1007/s10973-011-2153-x

Poletto, M., Ornaghi, H. L., & Zattera, A. J. (2014). Native cellulose: structure, characterization and thermal properties. *Materials*, *7*(9), 6105-6119. doi: 10.3390/ma7096105

Pracella, M., Haque, M. M. U., & Puglia, D. (2014). Morphology and propertiestuning of PLA/cellulose nanocrystals bio-nanocomposites by means of reactive functionalization and blending with PVAc. *Polymer, 55*(16), 3720-3728. doi: 10.1016/j.polymer.2014.06.071

Pracella, M., Haque, M. M., & Alvarez, D. P. V. (2012). Preparation and characterization of PLA nanocomposites with nanocellulose filled PVAC. *The European conference on composite materials*, 24-28.

Rambabu, N., Panthapulakkal, S., Sain, M., & Dalai, A. K. (2016). Production of nanocellulose fibers from pinecone biomass: evaluation and optimization of chemical and mechanical treatment conditions on mechanical properties of nanocellulose films. *Industrial Crops and Products*, *83*, 746-754. doi: 10.1016/j.indcrop.2015.11.083

Ramires, E. C., & Dufresne, A. (2012). Cellulose nanoparticles as reinforcement in polymer nanocomposites. In *Advances in Polymer Nanocomposites* (pp. 131-163). doi: 10.1533/9780857096241.1.131

Rattanapoltee, P., & Kaewkannetra, P. (2014). Utilization of agricultural residues of pineapple peels and sugarcane bagasse as cost-saving raw materials in *Scenedesmusacutus*for lipid accumulation and biodiesel production. *Applied Biochemistry and Biotechnology*, *173*(6), 1495-1510. doi: 10.1007/s12010-014-0949-4

Roman, M., & Winter, W. T. (2004). Effect of sulfate groups from sulfuric acid hydrolysis on the thermal degradation behavior of bacterial cellulose. *Biomacromolecules, 5*(5), 1671-1677. doi: 10.1021/bm034519+

Roumeli, E., Papadopoulou, E., Pavlidou, E., Vourlias, G., Bikiaris, D., Paraskevopoulos, K. M., & Chrissafis, K. (2012). Synthesis, characterization and thermal analysis of urea–formaldehyde/nanoSiO 2 resins. *Thermochimica Acta*, *527*, 33-39. doi: 10.1016/j.tca.2011.10.007

Rowe, A. A., Tajvidi, M., & Gardner, D. J. (2016). Thermal stability of cellulose nanomaterials and their composites with polyvinyl alcohol (PVA). *Journal of Thermal* Analysis and Calorimetry, 126(3), 1371-1386. doi: 10.1007/s10973-016-5791-1

Saddawi, A., Jones, J. M., Williams, A., & Wojtowicz, M. A. (2009). Kinetics of the thermal decomposition of biomass. *Energy & Fuels, 24*(2), 1274-1282. doi: 10.1021/ef900933k

Shahabi-Ghahafarrokhi, I., Khodaiyan, F., Mousavi, M., & Yousefi, H. (2015). Preparation and characterization of nanocellulose from beer industrial residues using acid hydrolysis/ultrasound. *Fibers and Polymers, 16*(3), 529. doi: 10.1007/s12221-015-0529-4

Thakur, V. K. & Singha, A. S. (2010). Natural fibres-based polymers—part i—mechanical analysis of pine needles reinforced biocomposites. *Bulletin of Materials Science, 33(*3), 257–264. doi: 10.1007/s12034-010-0040-x

Thakur, V. K., Thakur, M. K., & Gupta, R. K. (2013). Graft copolymers from cellulose: synthesis, characterization and evaluation. *Carbohydrate Polymers*, *97*(1), 18-25. doi: 10.1016/j.carbpol.2013.04.069

Veigel, S., Müller, U., Keckes, J., Obersriebnig, M., & Gindl-Altmutter, W. (2011). Cellulose nanofibrils as filler for adhesives: effect on specific fracture energy of solid wood-adhesive bonds. *Cellulose*, *18*(5), 1227. doi: 10.1007/s10570-011-9576-1

Zhang, H., Zhang, J., Song, S., Wu, G., & Pu, J. (2011). Modified nanocrystalline cellulose from two kinds of modifiers used for improving formaldehyde emission and bonding strength of urea-formaldehyde resin adhesive. *BioResources*, *6*(4), 4430-4438.

Zorba, T., Papadopoulou, E., Hatjiissaak, A., Paraskevopoulos, K., & Chrissafis, K. (2008). Urea-formaldehyde resins characterized by thermal analysis and FTIR method. *Journal of Thermal Analysis and Calorimetry, 92*(1), 29-33. doi: 10.1007/s10973-010-1143-8

Artículo 2:

European Pallets Fabricated with Composite Wood Blocks from Tropical Species Reinforced With Nanocrystalline Cellulose (NCC): Effect on the Properties of Blocks and Static Flexure of the Pallet

Priscilla Rigg-Aguilar[a], Róger Moya[a]*, José Vega-Baudrit[b], Angel Navarro-Mora[c], Johana Gaitan-Alvarez

The objective of the present study was to characterize the performance of composite wood blocks (CWB) by testing internal bond, nail extraction and water absorption. CWR was glued with two wood adhesives —polyvinyl acetate (PVAc) and urea formaldehyde (UF)— modified with 1% nanocrystalline cellulose (NCC). Three tropical species were employed: *Vochysia ferruginea*, *Cordia alliodora* and *Gmelina arborea*. In addition, the original European pallet in the static flexure test was evaluated. The results showed that the internal bond relative to solid wood blocks (SWB) increased with both adhesives. On the other hand, CWB of *V. ferruginea* with UF and *C. alliodora* with PVAc showed the highest resistance to nail extraction, while in *G. arborea*, the NCC increased the resistance to nail extraction. CWB with modified adhesives absorbed more moisture, particularly with PAVc, compared to SWB. Regarding the static flexure in pallets fabricated with of CWB, the load at the limit of proportionality and the maximum load increased, while deflections were lower in relation to SWB. The results show the potential of utilizing NCC in CWB fabricated with tropical species.

Keywords: nanocrystalline cellulose, adhesives, wood, composite blocks, pallets

*a: Escuela de Ingeniería Forestal, Instituto Tecnológico de Costa Rica, Cartago, Costa Rica. Apartado 159-7050, b: Laboratório Nacional Nanotecnologia (LANOTEC), Centro Nacional de Alta Tecnologia-CENAT, San Jose, Costa Rica. c: Escuela de Ingeniería en Construcción, Instituto Tecnológico de Costa Rica, Cartago, Costa Rica; *Corresponding author: rmoya@itcr.ac.cr*

INTRODUCTION

Cellulose is the most abundant organic compound in the planet (Thakur *et al*. 2013). It is a polymer naturally formed by all plants, together with other also important components, such as lignin, hemicelluloses and waxes (Li *et al*. 2009). Cellulose can be found all over the plant, although it is mostly concentrated in the stem (Lavoine *et al*. 2012) to support the plant (Morán *et al*. 2008).

As a renewable material and because of its physical and chemical characteristics, cellulose has become of great interest for the production of materials in the last decades (Poletto *et al*. 2014). With dimensions of 20 nanometers in diameter and 100-400 nanometers in length, products such as micro fibrillated cellulose (MFC) and nanocrystalline cellulose (NCC) can be obtained from it (Morán *et al*. 2008). MFC and NCC have been studied and used as reinforcements and filling in various polymers (Poletto *et al*. 2014) due to the strength properties conferred by its crystalline nature (Atta-Obeng *et al*. 2013), low molecular weight and biodegradability (Liew *et al*. 2015).

On the other hand, wood is a renewable material with good structural resistance that competes with other non-renewable materials (Tsoumis 2013). However, wood has the inconvenient that over 40% of the raw material turns into wastes during the industrialization process and can become a problem unless adequate management measures are taken, particularly in underdeveloped countries like Costa Rica (Gaitán-Álvarez *et al*. 2017). Some industries in more industrialized countries employ wood wastes as raw material to develop other products, such as wood composites or for energy production (Thakur *et al*. 2014).

Added to problem of wastes from the wood industry in Costa Rica, is the problem of stubble from pineapple plantations. The annual pineapple (*Ananas comosus*) world crop, of around 24.8 million tons

(Darnaudery *et al*. 2018) produces large amounts of residues in the form of unused leaves, stems, crowns and fruit peel (Rattanapoltee and Kaewkannetra 2014). Nearly 300 tons stubble per pineapple-sown hectare are produced in Costa Rica (Moya *et al*. 2016), where these wastes, as in other countries, have not yet received adequate management (Moya and Camacho 2014). Because this is a slow-decaying material, toxic herbicides such as N, N-dimethyl-4,4-bipyridinium dichloride (Paraquat) are commonly used; Paraquat is a soil contaminating herbicide with accumulative toxicity (Moya *et al*. 2016).

One possible application for the pineapple wastes is the extraction of natural fibers for manufacturing ropes and textiles, among other products (Moya and Camacho 2014), or for pulp production (Moya *et al*. 2016). However, recent research presents the possibility of extracting nanocrystalline cellulose from the pineapple fibers with the purpose of reinforcing wood composites (Rigg-Aguilar *et al*. 2019; Balakrishnan *et al*. 2018).

Wood or pineapple residues can be converted into lignocellulosic composites, generally achieving better properties than solid wood. These composites are the result of particle bonding (Rowell, 2012) that increase their mechanical properties (Chaabouni and Boufi 2017; Moya *et al*. 2015a, 2015b). The final densities of the wood composites oscillate between 0.6 and 0.7 g cm^{-3} (Rangel *et al*. 2017). The particles are moistened with fillings or adhesives that increase their internal bond resistance, and are bonded by thermal pressure (Salari *et al*. 2013).

Several studies have shown that adding cellulose, either as NCC or MFC, to the two most important adhesives in the industry of adhesives (urea-formaldehyde and polyvinyl acetate), improves the performance of the adhesive in lignocellulosic composites, wood composites in this case (Aydemir 2014; Ayrilmis *et al*. 2016; Chaabouni and Boufi 2017; Mahrdt *et al*. 2016; Kwon *et al*. 2015; Thakur and Singha 2010).

Despite the advances in the production of wood composites in Costa Rica, the development of composite-based products is limited. Consequently, use of wastes is scarce (Serrano and Moya 2012). Therefore, an important market for composites can be visualized in this country. For example, 50% timber consumption in Costa Rica is destined to pallet fabrication (Oficina Nacional Forestal [ONF] 2017) utilizing woody species such as *Gmelina arborea*, *Cordia alliodora* and *Vochysia ferruginea* (Rigg-Aguilar *et al*. 2019).

As for pallet production, a high percentage are European type, fabricated with blocks 10 cm x 10 cm x 10 cm obtained from logs with diameters greater than 20 cm (Rigg-Aguilar *et al*. 2019). This log dimension is large for the diameters produced in fast growth forest plantations in Costa Rica (Serrano and Moya 2012). Therefore, producers are worried seeking alternatives for producing blocks from wood composites or other lignocellulosic materials (Zivic *et al*. 2017), considering that there are experiences in other countries regarding pallet manufacturing using blocks produced with wood wastes (Kain *et al*. 2013; Zivic *et al*. 2017).

For the above reasons there is interest in the Costa Rican industry to fabricate composite wood blocks (CWB) to make European type pallets from timber and pineapple residues, by extracting the NCC and applying it to the adhesives. Therefore, the objective of this work was to characterize CWB and used for European type pallet fabrication, utilizing three tropical forest species (*Cordia alliodora*, *Gmelina arborea* and *Vochysia ferruginea*) glued with two adhesives, polyvinyl acetate and urea formaldehyde, modified with 1% nanocrystalline cellulose, by applying the tests internal bond resistance, nail extraction and water absorption; additionally, to evaluate the static flexure of European pallets fabricated with CWB.

EXPERIMENTAL

Material

The nanocrystalline cellulose (NCC) was provided by the Laboratorio Nacional de Nanotecnología (LANOTEC). It was extracted from pineapple (*Ananas comosus*) peel through a two-stage acid hydrolysis process. NCC sizes were between 20-40 nm in diameter (Camacho *et al*. 2017) and its concentration was 0.66 g ml-1. The details of the extraction and characterization can be found in Rigg-Aguilar *et al*. (2019).

Two adhesive types were employed: polyvinyl acetate (PVAc) and urea formaldehyde (UF). PVAc is a Resistol M.R. 850 water-based adhesive produced by Henkel Capital S.A. (http://www.resistol.com.mx/es.html). The technical description of the product indicates that the resin is water-based PVAc, with 54.5-55% solid contents and between 1600-2000 cPs viscosity. The UF adhesive is also water-based, of the brand Resina CR-560 U-F, manufactured by Química Centroamericana, Quibor, S.A. (http://www.agroquibor.com/). The UF adhesive has four components: resin (51%), water (26%), wheat flour

as agglutinant (20%), and ammonium sulphate as catalyser (3%). The technical description indicates that the pure resin contains 64-65% solid contents and 650-900 cPs viscosity. The total solid contents of the complete adhesive with the four components is 48%.

The wood used to evaluate the effect of nanocellulose in the two adhesives came from three tropical plantation species in Costa Rica: *Gmelina arborea* Roxb. (melina), *Vochysia ferruginea* Mart (botarrama) and *Cordia alliodora* Ruiz & Pav. (laurel), the three of them commonly used for pallet fabrication (ONF, 2017) and commercially important in Costa Rica (Tenorio *et al*. 2016).

The wood utilized came from plantations with ages ranging between 7 and 9 years: *C. alliodora* came from CATIE-Turrialba (latitude: 09°53'00''N and longitude: 83°38'01'' W, at an altitude of 602 masl, 9 years old); *G. arborea* came from Bonifacio, Limón (latitude: 09°46' 43'' N and longitude: 82°54' 59'' W, 42 masl and 8 years old) and *V. ferruginea* came from Búfalo-Limón (latitude: 10°00'21'' N and longitude: 83°10'23'' W, at 25 masl and 7 years old). Between 7 and 8 trees per species were felled. In the case of the pallets fabricated with solid wood, *G. arborea* from the plantation above described was utilized.

Nanocrystalline Cellulose (NCC) in Wood Adhesives

We evaluated the effect of 1% concentration NCC in the two wood adhesives (PVAc and UF), according to the results obtained by Rigg-Aguilar *et al*. (2019). The 1% concentration (weight weight^{-1}) was added according to the percentage of solids in each adhesive (55% for PVAc and 48% for UF).

The mixture of NCC with adhesives was prepared as follows: (i) 150 grams of PVAc were placed into a recipient and stirred with an inclined-blade agitator (45°) at 1600 rpm; then, the proportion of NCC gel (approximately 12.5 ml for 1% concentration) was slowly added into the adhesive. Stirring of the NCC-adhesive mixture continued for 10 minutes; (ii) as for UF, since this adhesive has 4 components (resin, water, wheat flour and ammonium sulphate as catalyser), 76.5 g of the resin were initially mixed with 10.9 ml NCC and stirred for 5 minutes at 1600 rpm with an inclined-blade agitator (45°), and then the rest of the components were added (33.55–28.10 ml of water, respectively, 30 g flour and 4.5 ml catalyser), while stirring continued during 5 additional minutes.

Effect of the NCC in Composite Wood Blocks for Making European Pallets

In the first stage we tested flexure in European pallets, using CWB with 1% NCC concentration and CWB fabricated with particles from *G. arborea*, *V. ferruginea* and *C. alliodora*. In the second stage, we evaluated only CWB fabricated with particles of three species using both adhesives and 1% NCC concentration, in the following tests: (i) internal bond; (ii) resistance to extraction of pallet nails; and (iii) percentage of water absorption. In addition, the CWB fabricated with 1% NCC concentration were compared in the same tests with blocks fabricated with adhesive without NCC and with SWB of the same species evaluated.

Composite Wood Blocks Manufacturing

The dimensions of the CWB were 10 cm x 10 cm x 10 cm and were composed of wood particles from *V. ferruginea*, *C. alliodora* and *G. arborea*, employing NCC-modified adhesive. Firstly, we obtained chips from 60 logs 1 m long and variable diameter of the three species. The chips were grinded and the material was sieved to obtain sizes between 3 mm and 10 mm, with moisture contents between 2–4%.

We took 550 g dry particles and mixed them with 100 g NCC-modified adhesive (18% total chip weight) for UF and 66 g (12% of total chip weight) for PVAc. The adhesive was slowly added to the particles while stirring during four minutes (Figure 1a). The glued particles were placed into a mould and pressed for 5 minutes with a 60 tonnes capacity Tinus Olsen universal testing machine (Fig. 1b). The mould was then heated to reach 180°C, while pressure was applied during 60-75 minutes to obtain the CWB (Fig. 1c). Lastly, CWB were conditioned to 12 % moisture content for two weeks.

We fabricated 72 CWB (2 adhesives x 2 concentrations (1% and 0%) x 9 blocks per pallet x 2 samples) that we used to fabricate the pallets for each species, and then the same amount of blocks (2 adhesives x 2 concentrations (1% and 0%) x 9 blocks per pallet x 2 samples) to perform the tests with the composite wood with modified adhesive.

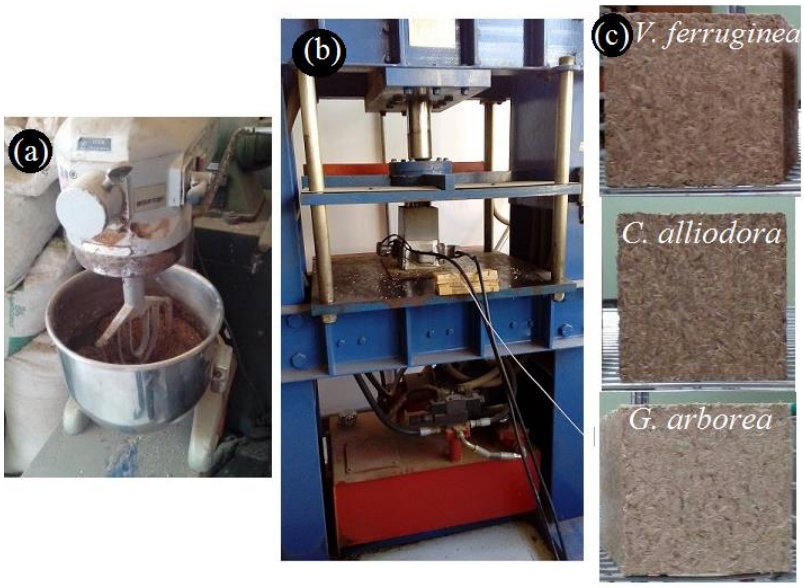

Fig. 1. Process of fabrication of the composite wood blocks for European pallets utilizing 1% NCC in PVAc and UF adhesives

Internal Bond and Perpendicular Tension Resistance in Composite Wood Blocks

We cut five different CWB fabricated with the two adhesives and modified with 1% NCC, according to Fig. 2c, obtaining 4 samples of 5 cm x 5 cm x 10 cm per block. Thus, 20 samples per treatment were obtained (2 adhesives: NCC-modified and NCC-un-modified). The internal bond test was performed in accordance with the ASTM D1037-12 (ASTM 2018a) standard. The bonding strength of the CWB was compared with the grain-perpendicular tension strength of the SWB (Figure 2d). To this purpose, we obtained SWB in green condition for European pallets from Maderas Bosque Verde S.A. (https://www.facebook.com/MaderasBosqueVerde/). The SWB were cut according to Fig. 2b and 8 samples of 5 x 5 x 6.3 cm were extracted (Figure 2d). Therefore, 24 samples per treatment were tested, following the ASTM D143-14 (ASTM 2018b).

Resistance to Nail Extraction in Composite Wood Blocks

Then, 5 CWB (10 cm x 10 cm x 10 cm) with both adhesives (PVAc and UF) and 1% NCC-modified, and unmodified (0% NCC), and 5 SWB from each species were utilized to measure the resistance to nail extraction. In both cases the ASTM D1761-12 (ASTM 2018c) standard was followed, inserting pallet nails 5 cm long, 12.5 caliber and a 32º-angle spiral, to a depth of 32 mm at each side of the block, with a minimum distance between the nails and the edge of the block of 2.54 cm. Nails are inserted on all sides of the blocks, to determine the lateral and transverse resistance. As for the composite wood blocks, the transverse directions were defined as the sections where compression was exerted, while the lateral directions were the sections perpendicular to the direction of the compression force at the time of block fabrication. The number of tests per treatment were 30.

Water Absorption

Samples sized 5 cm x 5 cm x 2.54 cm were extracted from the 5 conditioned CWB per treatment (Fig. 1e). The samples were placed vertically into trays with water covering the bottom up to 2.54 cm during 24 hours, in accordance with ASTM D1037-12 (ASTM 2018d). The weight was recorded before placing into water and after 24 hours. Water absorption was calculated for each one of the samples according to the ratio water absorbed and sample weight, before the absorption test, expressed as a percentage.

Pallet Fabrication

The pallets were fabricated at Maderas Bosque Verde S.A. (https://www.facebook.com/MaderasBosqueVerde/). The dimensions of the European pallet were 1.10 m long, 0.98 m wide and 15 cm high (Fig. 2a). The upper boards were 10.1 mm wide and 1.8 mm thick; 7 boards were placed. In both cases, *G. arborea* was utilized. The pallets were nailed employing a 6 bar pressure pneumatic pistol, 2 nails 5 cm long, 12.5 caliber and 32º-angle spiral. The lower side of the pallet featured 3

G. arborea boards supporting the blocks and 3 boards perpendicular to the first 3, measuring 8.3 mm wide and 1.8 mm thick. Each block was nailed with two nails to the lower boards.

Static Flexure of the Complete Pallet

The pallets fabricated with CWB, as well as the SWB were tested for flexural strength according to the ISO 8611-1 (ISO 2013), in which the pallet is placed on its sides, while a double load is applied on the sections between the blocks (Fig. 2b) at 60 N per minute. A crackmeter sensor was placed at each side of the pallet to measure the vertical deflection at the central section of the pallet. During the test, the load and the deflection were recorded in periods of 4 seconds until the pallet failed. These data were utilized to calculate the load and deflection at the limit of proportionality (L_{LP} and D_{LP}) and the maximum load and deflection (L_{max} and D_{max}) of the pallet based on the calculations of ISO 8611-1 (ISO 2013). At the end of the test we recorded the different types of failure occurring to the pallet.

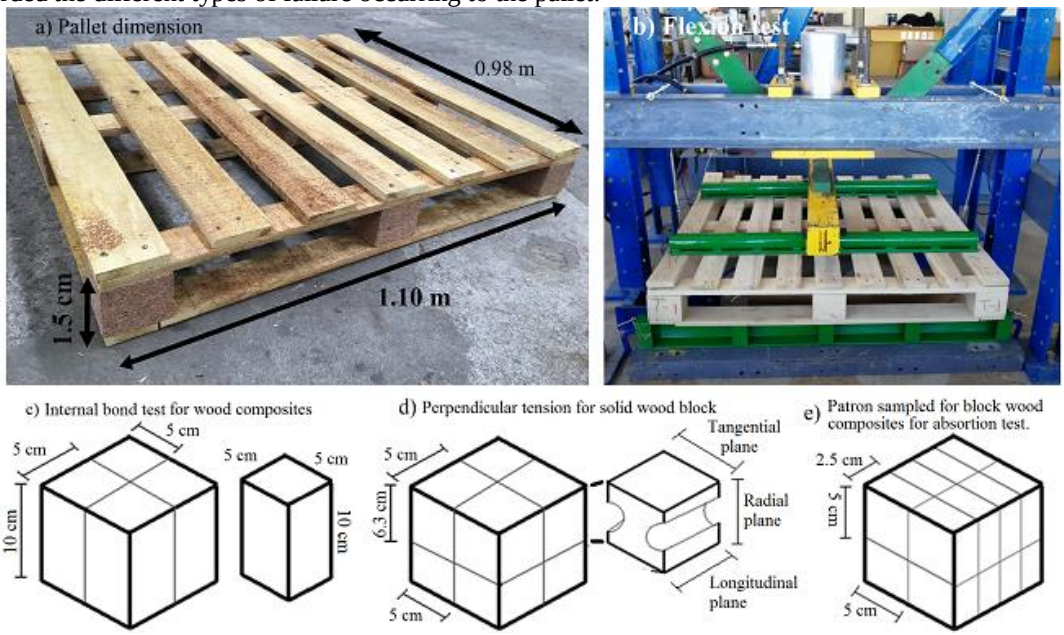

Fig. 2. (a) Dimensions and aspect of the pallet fabricated with composite wood; (b) pallet flexural test and cutting patterns to obtain the samples for tests; (c) internal bond; (d) perpendicular tension in solid wood blocks and (b) water absorption.

Statistical analysis

We evaluated the assumptions of normal data distribution by means of the Shapiro Wilk test and the variance homogeneity with the Levene test and the InfoStat software. Then, to determine the differences between the means of the tests, an ANOVA test was applied, where the tests performed were the response variables and the NCC concentration was the independent variable. Then, this analysis was accompanied by the Tukey test at 99% reliability to determine the differences between both NCC concentrations within the species per adhesive. As the internal bond and water absorption tests did not meet the assumptions, we used non-parametric tests; the Kruskal Wallis test to determine differences between NCC concentrations, and the Steel test to compare the composite blocks with the control treatment (solid wood blocks).

RESULTS AND DISSCUSION

Evaluation of the composite wood blocks regarding internal bond resistance and resistance to nail extraction

Table 1 shows the internal bond resistance of the blocks used for pallets. Comparing with tension parallel to the grain, the SWB show statistically greater internal bond resistance values than the values shown by CWB with unmodified adhesive and with NCC-modified adhesive in the three species. Modifying the adhesive with NCC does not affect the value of strength of the internal bond resistance of CWB fabricated with PVAc, as no significant differences are observed in the three species between adhesives with or without NCC. In contrast, in CWB fabricated with UF adhesive and modified with 1% NCC, the internal bond resistance increased significantly in relation to CWB fabricated with unmodified adhesive (Table 1).

As regards resistance to nail extraction, the analysis between NCC concentrations of the CWB for each species per adhesive showed that, for *C. alliodora* and *G. arborea* with PVAc adhesive, a resistance increase in both sections was observed for nail extraction with 1% NCC, which is statistically different only in the case of the lateral section in *C. alliodora* (Table 1). In the rest of the cases neither reinforcement from NCC nor statistical differences were observed in most of the comparisons.

The CWB of *V. ferruginea* and *C. alliodora* glued with 1% NCC presented resistance to nail extraction statistically equivalent to SWB of *V. ferruginea* and *C. alliodora*, both laterally and transversally (Table 1). However, there was a slight increase in the resistance to nail extraction in CWB without NCC with both types of adhesives. In *G. arborea*, the SWB showed the highest value of resistance to nail extraction compared to CWB bonded with both adhesives, while the CWB with PVAc were statistically different from the control treatment.

Resistance in CWB is affected by varying aspects (Hoadley 2000; Carvalho *et al*. 2003), one of them is the size of the product, in this case, a 10 cm x 10 cm x 10 cm block, which is rather large to be densified by compression. Leng *et al*. (2017) and Vital *et al*. (1974) mention that the properties of the products increase their resistance if the material is adequately densified, especially if performed by compression, as were the blocks in this project. In addition, densification by compression at temperatures above 100 □C facilitates plasticization of the wood particles (Hunt *et al*. 2017), thus increasing the internal bond resistance. However, CWB cannot achieve the values observed for SWB (Rangel *et al*. 2017).

Table 1. Internal Bond -perpendicular Tension, Water Absorption, Pallet Nail Resistance, Moisture Content and Density in Blocks Used in European Pallets Fabricated With *V. ferruginea*, *C. alliodora* and *G. arborea* Particles Glued with PVAc and UF Adhesives With and Without NCC.

Species	Type of block (Adhesive - %NCC)		Internal bond resistance (MPa)	Water absorption (%)	Pallet nail resistance		Moisture content (%)	Density (g/cm^3)
					Lateral (N)	Transversal (N)		
V. ferruginea	Solid wood block (SWB)		2.09^{A} (0.771)	39.0^{A} (5.38)	398.4^{A} (92.0)	241.9^{A} (59.4)	18.38	0.30
	CWB with PVAc adhesive	0.0	0.14 ^{B}(0.041)	196.5^{B} (27.72)	370.2^{AB} (90.7)	252.5^{A} (47.0)	9.07	0.57
		1.0	0.16^{B} (0.049)	179.3^{B} (14.93)	285.3^{A} (73.9)	224.3^{A} (28.3)	8.28	0.58
	CWB with UF adhesive	0.0	0.07^{A} (0.033)	94.5^{A} (4.96)	532.5^{B} (60.9)	419.2^{B} (104.5)	10.03	0.62
		1.0	0.59^{B} (0.123)	131.2^{B} (11.47)	337.7^{A} (66.6)	176.1^{A} (35.8)	8.18	0.61
C. alliodora	Solid wood block (SWB)		1.89^{A} (0.622)	48.8^{A} (7.85)	391.3^{A} (119.2)	200.8^{A} (36.9)	17.05	0.31
	Composite block with PVAc adhesive	0.0	0.06^{B} (0.028)	251.5^{B} (27.25)	246.9^{B} (71.0)	82.7^{B} (25.6)	9.28	0.55
		1.0	0.06^{B} (0.013)	240.8^{B} (17.99)	393.5^{A} (96.5)	131.1^{B} (21.0)	8.19	0.57
	Composite block with UF adhesive	0.0	0.05^{A} (0.030)	120.0^{A} (9.43)	464.1^{A} (114.3)	285.6^{B} (63.7)	10.20	0.60
		1.0	0.22^{B} (0.058)	164.1^{B} (17.96)	308.0^{AB} (57.0)	192.3^{AB} (49.4)	7.47	0.61
G. arborea	Solid wood block (SWB)		2.00^{A} (0.654)	64.9^{A} (14.07)	437.3^{A} (125.4)	222.5^{A} (72.3)	40.87	0.39
	CWB with PVAc adhesive	0.0	0.01^{B} (0.003)	151.6^{B} (31.88)	107.3^{B} (36.6)	40.2^{B} (12.4)	11.00	0.56
		1.0	0.03^{B} (0.009)	176.7^{B} (27.26)	154.5^{B} (38.2)	65.7^{B} (20.4)	7.88	0.58
	CWB with UF adhesive	0.0	0.10^{B} (0.032)	67.5^{AB} (3.81)	251.0^{B} (48.7)	186.7^{A} (47.4)	10.83	0.62
		1.0	0.45^{A}(0.064)	100.6^{B} (8.70)	223.6^{B} (56.3)	173.5^{A} (43.5)	8.24	0.63

Legend: The values in parenthesis represent standard deviation. Average values identified with different letters are statistically different at α= 99%.

The increase in the internal bond resistance of the CWB with NCC- modified UF adhesive in the three species (Table 1) is supported by the works of Veigel *et al*. (2011) and Zhang *et al*. (2011), who found an increase in the internal bond resistance of the UF adhesive with added NCC. Kwon *et al*. (2015) mention that the increase in the resistance of NCC-modified adhesives is due to the fact that the cellulose fibres in the glue line merge with the adhesive inside the wood cavities, allowing better penetration; consequently, greater strength is needed to separate two wood pieces. Likewise, the reinforcement effect of the interface wood-adhesive is the result of the formation of a network between the NCC and the polymer chains of the adhesives (Grishkewich *et al*. 2017). Almeida et al. (2018) and Ramires and Dufresne (2012) explain that because the NCC has greater contact area, high resistance to traction and rigidity, allows the formation of a crystal network that interact with the adhesive, increasing its mechanical resistance.

On the other hand, in thermoplastic adhesives like PVAc, addition of NCC can improve the low rigidity of the polymers and adhesion in the glue line as well (Gindl-Altmutter and Veigel 2014). Different adhesion mechanisms occur within the interface wood particles and adhesives, since the adhesive can penetrate the wood, allowing interlinking and thus increasing internal adhesion. Moreover, internal strength within the adhesive allows the adhesive layer in the interface to remain bonded, improving the interactions and increasing the bonding strength (Gindl-Altmutter and Veigel 2014). This effect in the improvement of the properties can be observed in the addition of NCC into the PVAc adhesive in *V. ferruginea* and *G. arborea* with 1% NCC concentration (Table 1).

Modifying the PVAc adhesive with NCC did not improve the properties of the CWB (Table 1). Such result can be due to NCC producing a cracking effect inside the adhesive, decreasing the strength of the glue line (Gindl-Altmutter and Veigel 2014), which is reflected in the diminution of the resistance to nail extraction and of the internal bond strength of the blocks. Therefore, PVAc application to CWB has no beneficial effect on the bond resistance.

Water Absorption

CWB compared to SWB present higher water absorption percentage, being statistically equivalent in CWB with UF without NCC in the three species (Table 1). No statistical differences were observed regarding water absorption in CWB with the PVAc adhesive. Contrastingly, CWB with UF adhesive in *V. ferruginea* and *C. alliodora* present statistical differences between NCC concentrations, as water absorption is greater with 1% NCC concentration.

The hydrophobic nature and porous structure of the wood favour water absorption, since wood particles have a greater contact area (Salari *et al*. 2013). Added to this, neither of the two adhesives presented good performance against water (Yang *et al*. 2006), thus, greater water absorption in the CWB compared to SWB is expected (Table 1).

However, adding NCC to the PVAc adhesive improves block performance against water absorption. These results agree with Chaabouni and Boufi (2017) and Saad and Kamal (2015), who report that the decrease in water absorption in products using PVAc is explained by the interlinking between the OH groups with the adhesive matrix, preventing water intrusion inside the polymer matrix. In contrast, the same result cannot be obtained with the UF adhesive due to the reduced interaction between the NCC-modified adhesive and the wood particles that deteriorates the adhesion forces and prevents the formation of an adhesive barrier against water absorption, which results in increased amount of absorbed water (Almeida *et al*. 2018).

Noteworthy, composite wood blocks are affected by moisture content absorbed from the environment that impairs the performance of the composite, as moisture penetration can weaken the internal bonds of the wood particles (Rofii *et al*. 2016). CWB, once compressed, are extracted from the mould completely dry. During their conditioning the CWB absorb humidity from the environment, mainly in a tropical region such as Costa Rica. Due to water absorption, the CWB expand slightly, weakening the internal bonds of the adhesive or the wood-adhesive interface, or the resistance to nail extraction (Gerhards 2007).

Evaluation of the Pallets

The flexural test showed that L_{LP} and L_{max} increased for the pallets fabricated with CWB of the three species and with the two adhesives (PVAc and UF) modified with NCC at 1% (Table 2). The increase in LLP varied from 8% to 40%, while the increases in L_{max} ranged between 42% and 59%, with the lowest increase observed in *C. alliodora* and the highest in blocks fabricated with *V. ferruginea* (Table 2).

Table 2. Failure Types in *V. ferruginea*, *C. alliodora* and *G. arborea* Bonded With Adhesives Pvac And UF Under Two NCC Concentrations.

Parameter	Adhesive	Value	*Cordia alliodora*	*Gmelina arborea*	*Vochysia ferruginea*
Load at the limit of proportionality (kg)	SWB	1465			
	PVAc		1645 (12%)	1708 (17%)	2007 (40%)
	UF		1580 (8%)	1635 (12%)	1702 (16%)
Deflection at the limit of proportionality (mm)	SWB	28.5			
	PVAc		25.9 (-2,6)	27.1 (-1.4)	29.8 (+1.3)
	UF		25.4 (-3.1)	27.5 (-1.0)	28.7 (+0.2)
Maximum load (kg)	SWB	1556			
	PVAc		2377 (53%)	2392 (54%)	2483 (59%)
	UF		2202 (42%)	2428 (56%)	2258 (45%)
Maximum Deflection (mm)	SWB	31.24			
	PVAc		52.6 (+21.4)	48.7 (+17.5)	46.3 (+15.0)
	UF		49.4 (+18.2)	54.5 (+23.3)	45.7 (+14.5)

Legend: Values in parenthesis correspond to the percentage of load increase in the case of load at the limit of proportionality and maximum load. In the case of deflection, the values in parenthesis represent the deflection change of the pallet: "-", less deflection and "+", greater deflection.

Regarding the deflection values, D_{LP} was smaller for pallets fabricated with CWB of *C. alliodora* and *G. arborea* and the two nanocellulose modified adhesives. The decrease in D_{LP} ranged between 1.0 and 3.1 mm, and the lowest deflection values were observed in CWB of *C. alliodora*. In contrast, the pallets built with CWB of *V. ferruginea* presented higher D_{LP} than the pallets built with SWB. On the other hand, the D_{max} in pallets fabricated with the three species increased between 14.5 mm and 23.3 mm, while the greatest deflection was observed in pallets of *C. alliodora* and *G. arborea*, and the lowest deflection in pallets fabricated with *V. ferruginea* (Table 2).

Table 2 shows the behaviour of the load applied to the pallets fabricated with the different types of blocks (SWB or CWB) relative to deflection. In all the species, the load-deflection curves of the SWB pallets are below the load-deflection curves of the pallets constructed with CWB glued with two adhesives (PVAc and UF) modified with nanocellulose. This means that the pallets fabricated with these blocks manufactured with PVAc or UF modified with nanocellulose will present less deflection in relation to the pallets built of SWB, for the same load magnitude. Furthermore, these load-deflection curves also show that there is less deflection when using the UF adhesive in CWB, than in CWB glued with PVAC in *G. arborea* (Fig. 2b) and *V. ferruginea* (Fig. 2c). Meanwhile, the deflection for the same load in the wooden blocks of *C. alliodora* is similar in the two adhesives tested (Fig. 2c).

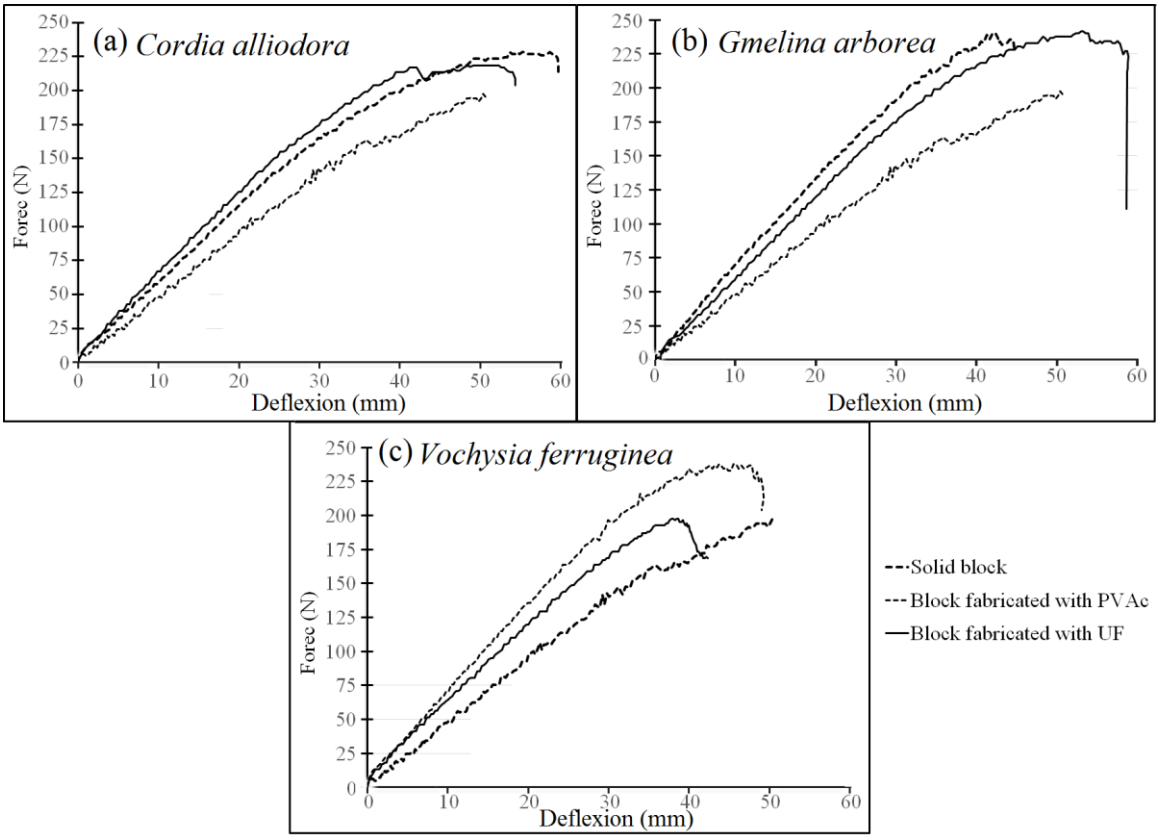

Fig. 2. Load curve vs deflection in the flexural test in pallets fabricated with composite wood blocks of *Cordia alliodora* (a), *Gmelina arborea* (b) and *Vochysia ferruginea* (c) with two different wood adhesives.

In relation to the type of failure, the pallets constructed with CWB of the three species presented the same failures shown by SWB pallets. The failure types were: (i) type I: upper boards detached at the corners of the pallets, both from the lower boards and from the blocks themselves (Fig. 3a-b); (ii) type II: upper board broken (Fig. 3c), (iii) type III: failure caused by tension in the lower boards of the central block of the pallet (Fig. 3d) and (iv) type IV: internal block bonding (Fig. 3d). Most pallets presented failure type I (Fig. 3a). Only one pallet fabricated with composite *V. ferruginea* blocks and another pallet built with composite *C. alliodora* blocks presented failure types II and IV (Fig. 3c-3d), respectively. As for the two pallets fabricated with CWB of *G. arborea* with the NCC-modified PVAc adhesive, the blocks failed due to internal bond (Fig. 3d).

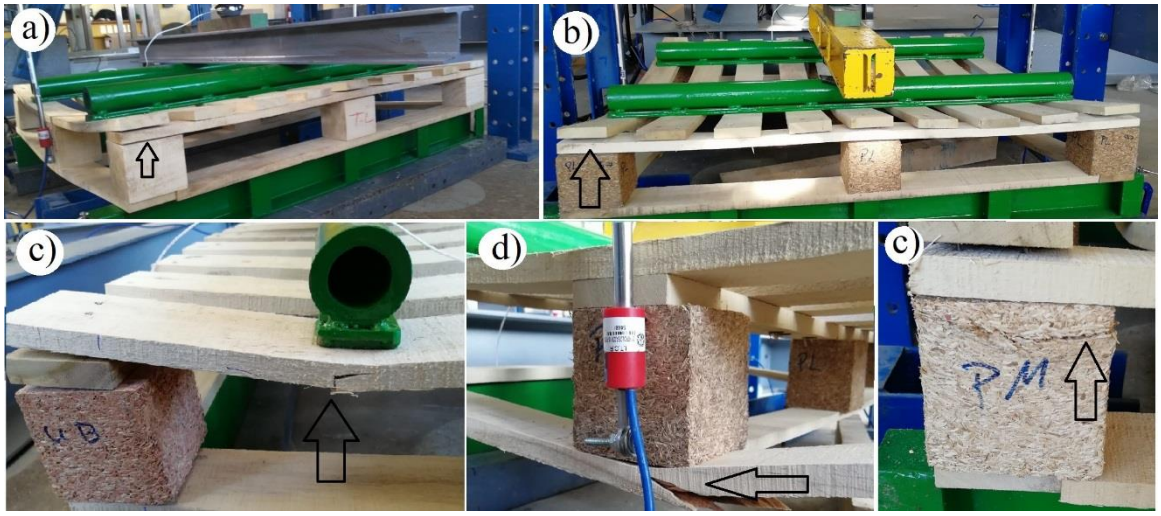

Fig. 3. Types of failures in pallet flexural tests: (i) Type I: upper boards detached (a-b). (ii) Type II: upper board broken (c); (iii) type III: failure due to tension (c) and (iv) type IV: failure due to internal block bonding (d).

CONCLUSIONS

1. The addition of 1% NCC to PVAc and UF in CWB of *Vochysia ferruginea*, *Cordia alliodora* and *Gmelina arborea* to produce European pallets showed an increase in the internal bond of the block in the nail extraction test. Therefore, the NCC improves the resistance properties of wood adhesives. However, although the level of water absorption diminished with added NCC, it remained higher than in SWB, which should be taken into account in pallet fabrication using CWB.

2. CWB produced using NCC-modified PVAc and UF and the wood from the tropical species commonly used for pallet fabrication in Costa Rica improves the performance of the static flexure of the European pallet, specifically, the values of maximum load and deflection. This result, together with the tests conducted on CWB, indicates that substituting the SWB for a CWB and adding 1% NCC to the adhesives is a viable option that improves the structural performance of the European pallet.

ACKNOWLEDGMENTS

The authors wish to thank the Vicerrectoría de Investigación y Extensión at the Instituto Tecnológico de Costa Rica for their assistance in conducting this study.

REFERENCES CITED

Almeida, R.G., Mendes, L.M., Sanadi, A.R., de Sena Neto, A.R., Claro, P.I.C., Corrêa, A. C., and Marconcini, J.M. (2018) Urea formaldehyde and cellulose nanocrystals adhesive: studies applied to sugarcane bagasse particleboards," *Journal of Polymers and the Environment*, 26(7), 3040-3050. doi: 10.1007/s10924-018-1189-4

ASTM D1037-12 (2018a). "Standard test methods for evaluating properties of wood-base fiber and particle panel materials" American Society for Testing and Materials, West Conshohocken, PA.

ASTM D143-14 (2018b). "Standard test methods for small clear specimens of timber," American Society for Testing and Materials, West Conshohocken, PA.

ASTM D1761-12 (2018c). "Standard test methods for mechanical fasteners in wood" American Society for Testing and Materials, West Conshohocken, PA.

Atta-Obeng, E., Via, B.K., Fasina, O., Auad, M.L., and Jiang, W. (2013). "Cellulose reinforcement of phenol formaldehyde: Characterization and chemometric elucidation," *International Journal of Composite Materials* 3(3), 61-68. doi: 10.5923/j.cmaterials.20130303.04

Aydemir, D. (2014). "The lap joint shear strength of wood materials bonded by cellulose fiber-reinforced polyvinyl acetate," *BioResources* 9(1), 1179-1188.

Ayrilmis, N., Kwon, J.H., Lee, S.H., Han, T.H., and Park, C.W. (2016). "Microfibrillated-cellulose-modified urea-formaldehyde adhesives with different F/U molar ratios for wood-based composites," *Journal of Adhesion Science and Technology* 30(18), 2032-2043. doi: 10.1080/01694243.2016.1175246

Berrocal, A., Gaitan-Alvarez, J., Moya, R., Fernández-Sólis, D. and Ortiz-Malavassi, E. (2019) "Development of heartwood, sapwood, bark, pith and specific gravity of teak (*Tectona grandis*) in fast-growing plantations in Costa Rica," *Journal of Forest Research* DOI: https://doi.org/10.1007/s11676-018-0849-5

Balakrishnan, P., Gopi, S., Geethamma, V. G., Kalarikkal, N., and Thomas, S. (2018) "Cellulose nanofiber vs nanocrystals from pineapple leaf fiber: a comparative studies on reinforcing efficiency on starch nanocomposites". *Macromolecular Symposia* 380(1), 1800102. doi: 10.1002/masy.201800102

Camacho, M., Ureña, Y.R.C., Lopretti, M., Carballo, L.B., Moreno, G., Alfaro, B., and Baudrit, J. R. V. (2017) "Synthesis and characterization of nanocrystalline cellulose derived from pineapple peel residues," *Journal of Renewable Materials*, 5(3-4), 271-279. doi: 10.7569/JRM.2017.634117

Carvalho, L.M.H., Costa, M.R.N., and Costa, C.A.V. (2003) "A global model for the hot-pressing of MDF," *Wood Science and Technology* 37(3-4), 241-258. doi: 10.1007/s00226-003-0170-z

Chaabouni, O., and Boufi, S. (2017) "Cellulose nanofibrils/polyvinyl acetate nanocomposite adhesives with improved mechanical properties," *Carbohydrate Polymers* 156, 64-70. doi: 10.1016/j.carbpol.2016.09.016

Darnaudery, M., Fournier, P., and Lechaudel, M. (2018). "Low-input pineapple crops with high quality fruit: Promising impacts of locally integrated and organic fertilisation compared to chemical fertilisers" *Experimental Agriculture* 54(2), 286-302. doi: 10.1017/S0014479716000284

Gaitán-Alvarez, J., Moya, R., Rodríguez-Zúñiga, A., and Puente-Urbina, A. (2017). "Characterization of torrefied biomass of five reforestation species (*Cupressus lusitanica, Dipteryx panamensis, Gmelina arborea, Tectona grandis, and Vochysia ferruginea*) in Costa Rica," *BioResources*, 12(4), 7566-7589.

Gerhards, C.C. (2007). "Effect of moisture content and temperature on the mechanical properties of wood: an analysis of immediate effects," *Wood and Fiber Science* 14(1), 4-36.

Gindl-Altmutter, W., and Veigel, S. (2014). "Nanocellulose-modified wood adhesives. In *Handbook of Green Materials: 2 Bionanocomposites: processing, characterization and properties* (pp. 253-264). doi: 10.1142/9789814566469_0031

Grishkewich, N., Mohammed, N., Tang, J., and Tam, K. C. (2017) "Recent advances in the application of cellulose nanocrystals," *Current Opinion in Colloid & Interface Science* 29, 32-45. doi: 10.1016/j.cocis.2017.01.005

Hoadley, R.B. (2000). *Understanding wood: a craftsman's guide to wood technology*. Taunton press.

Hunt, J.F., Leng, W., and Tajvidi, M. (2017). "Vertical density profile and internal bond strength of wet-formed particleboard bonded with cellulose nanofibrils," *Wood and Fiber Science* 49(4), 1-11.

ISO 8611-1 (2013). "Pallet for materials handling – Flat pallets – Part 1: test methods" International Standard. Geneva, Italy.

Kain, G., Heinzmann, B., Barbu, M. C., and Petutschnigg, A. (2013). "Softwood bark for modern composites". *Pro Ligno* 9(4), 460-468.

Kwon, J. H., Lee, S. H., Ayrilmis, N., and Han, T. H. (2015). "Tensile shear strength of wood bonded with urea–formaldehyde with different amounts of microfibrillated cellulose," *International Journal of Adhesion and Adhesives* 60, 88-91. doi: 10.1016/j.ijadhadh.2015.04.002

Lavoine, N., Desloges, I., Dufresne, A., and Bras, J. (2012). "Microfibrillated cellulose–Its barrier properties and applications in cellulosic materials: A review," *Carbohydrate Polymers* 90(2), 735-764. doi: 10.1016/j.carbpol.2012.05.026

Leng, W., Hunt, J.F., and Tajvidi, M. (2017). "Effects of density, cellulose nanofibrils addition ratio, pressing method, and particle size on the bending properties of wet-formed particleboard," *BioResources* 12(3), 4986-5000. doi : 10.15376/biores.12.3.4986-5000

Li, R., Fei, J., Cai, Y., Li, Y., Feng, J., and Yao, J. (2009). "Cellulose whiskers extracted from mulberry: A novel biomass production," *Carbohydrate Polymers* 76(1), 94-99. doi: 10.1016/j.carbpol.2008.09.034

Liew, F.K., Hamdan, S., Rahman, M.R., Rusop, M., Lai, J.C.H., Hossen, M.F., and Rahman, M.M. (2015) "Synthesis and characterization of cellulose from green bamboo by chemical treatment with mechanical process," *Journal of Chemistry* 2015, Article ID 212158, 6 pages, doi: 10.1155/2015/212158

Mahrdt, E., Pinkl, S., Schmidberger, C., van Herwijnen, H.W., Veigel, S., and Gindl-Altmutter, W. (2016). "Effect of addition of microfibrillated cellulose to urea-formaldehyde on selected adhesive characteristics and distribution in particleboard," *Cellulose* 23(1), 571-580. doi: 10.1007/s10570-015-0818-5

Morán, J.I., Álvarez, V.A., Cyras, V.P., and Vázquez, A. (2008). "Extraction of cellulose and preparation of nanocellulose from sisal fibers," *Cellulose* 15(1), 149-159. doi: 10.1007/s10570-007-9145-9

Moya, R, Camacho, D (2014) "Production of natural fiber obtained from the leaves of pineapple plants (*Ananas comosus*) cultivated in Costa Rica" in: Biomass and Bioenergy-Processing and Properties, Rehman K, Mohammad J, Umer R, Springer, New York, USA, pp. 111-124.

Moya, R, Berrocal, A, Rodriguez-Zuñiga, A, Rodriguez-Solis, M, Villalobos-Barquero, V, Starbird, R, Vega-Baudrit, J (2016) "Biopulp from pineapple leaf fiber produced by colonization with two white-rot fungi: *Trametes versicolor* and *Pleurotus ostreatus*," *BioResources* 11(4), 8756-8776.

Moya, R., Rodríguez-Zúñiga, A., and Vega-Baudrit, J. (2015a). "Effects of adding multiwall carbon nanotubes on performance of polyvinyl acetate and urea-formaldehyde adhesives in tropical timber species," *Journal of Nanomaterials* 16(1), 290. doi: 10.1155/2015/895650

Moya, R., Rodríguez-Zúñiga, A., Vega-Baudrit, J., and Álvarez, V. (2015b). "Effects of adding nano-clay (montmorillonite) on performance of polyvinyl acetate (PVAc) and urea-formaldehyde (UF) adhesives in *Carapa guianensis*, a tropical species," *International Journal of Adhesion and Adhesives* 59, 62-70. doi: 10.1016/j.ijadhadh.2015.02.004

Oficina Nacional Forestal [ONF] (2017). Estadísticas 2016. Usos y Aportes de la Madera en Costa Rica.

Poletto, M., Ornaghi, H. L., and Zattera, A. J. (2014). "Native cellulose: structure, characterization and thermal properties," *Materials* 7(9), 6105-6119. doi: 10.3390/ma7096105

Ramires, E.C., and Dufresne, A. (2012). "Cellulose nanoparticles as reinforcement in polymer nanocomposites". In *Advances in Polymer Nanocomposites* (pp. 131-163). doi: 10.1533/9780857096241.1.131

Rattanapoltee, P., and Kaewkannetra, P. (2014). "Utilization of agricultural residues of pineapple peels and sugarcane bagasse as cost-saving raw materials in *Scenedesmusacutus*for lipid accumulation and biodiesel production," *Applied Biochemistry and Biotechnology* 173(6), 1495-1510. doi: 10.1007/s12010-014-0949-4

Rangel, L., Moreno, P., Trejo, S., and Valero, S. (2017). "Propiedades de tableros aglomerados de partículas fabricados con madera de *Eucalyptus urophylla*," *Maderas. Ciencia y Tecnología* 19(3), 373-386 doi: 10.4067/S0718-221X2017005000032

Rigg-Aguilar, P., Moya, R., Vega-Baudrit, J., Gloria, O., Starbird, R., Puente-Urbina, A., Méndez, D., Potosme, LD and Esquivel, M. (2019). Micro- and nanofibrillated cellulose extracted from pineapple (*Ananas comosus*) stems and its application in polyvinyl acetate (PVAc) and urea-formaldehyde (UF) wood adhesives. *Cellulose* (submitted)

Rofii, M.N., Kubota, S., Kobori, H., Kojima, Y. and Suzuki, S. (2016). Furnish type and mat density effects on temperature and vapor pressure of wood-based panels during hot pressing. *Journal of Wood Science* 62(2), 168-173. doi: 10.1007/s10086-015-1531-6

Rowell, R.M. (Ed.). (2012). *Handbook of woodchemistry and wood composites*. CRC press.

Saad, M.J., and Kamal, I. (2015). Mechanical and physical properties of urea-formaldehyde bonded kenaf core particleboards. *Journal of Tropical Agriculture and Food Science* 41, 341-347.

Salari, A., Tabarsa, T., Khazaeian, A., and Saraeian, A. (2013). Improving some of applied properties of oriented strand board (OSB) made from underutilized low quality paulownia (*Paulownia fortunie*) wood employing nano-SiO_2. *Industrial Crops and Products* 42, 1-9. doi: 10.1016/j.indcrop.2012.05.010

Serrano-Montero, J. R., & Moya-Roque, R. (2012). Procesamiento, uso y mercado de la madera en Costa Rica: aspectos históricos y análisis crítico. *Revista Forestal Mesoamericana Kurú* ***8***(21), 1-12.

Tenorio, C., Moya, R., Salas, C., & Berrocal, A. (2016). Evaluation of wood properties from six native species of forest plantations in Costa Rica. *Bosque* 37(1),71-84 doi: 10.4067/S0717-92002016000100008

Thakur, V. K. and Singha, A. S. (2010). Natural fibres-based polymers—part i—mechanical analysis of pine needles reinforced biocomposites. *Bulletin of Materials Science* 33(3), 257–264. doi: 10.1007/s12034-010-0040-x

Thakur, V.K., Thakur, M.K. and Gupta R.K. (2013). Graft copolymers from cellulose: synthesis, characterization and evaluation. *Carbohydrate Polymers* 97(1), 18-25. doi: 10.1016/j.carbpol.2013.04.069

Thakur V.K., Thakur M.K., Raghavan, P. and Kessler, M.R. (2014). Progress in green polymer composites from lignin for multifunctional applications: a review. *ACS Sustainable Chemistry & Engineering* 2(5), 1072-1092. doi: 10.1021/sc500087z

Tsoumis, G. (2013). *Wood as raw material: source, structure, chemical composition, growth, degradation and identification*. Elsevier.

Veigel, S., Müller, U., Keckes, J., Obersriebnig, M., and Gindl-Altmutter, W. (2011). Cellulose nanofibrils as filler for adhesives: effect on specific fracture energy of solid wood-adhesive bonds. *Cellulose* 18(5), 1227-1231. doi: 10.1007/s10570-011-9576-1

Vital, B. R., Lehmann, W. F., and Boone, R. S. (1974). How species and board densities affect properties of exotic hardwood particleboards. *Forest Products Journal* 24(12), 37-45.

Yang, H.S., Kim, H.J., Park, H.J., Lee, B.J., and Hwang, T.S. (2006). Water absorption behavior and mechanical properties of lignocellulosic filler–polyolefin bio-composites. *Composite Structures* 72(4), 429-437. doi: 10.1016/j.compstruct.2005.01.013

Zhang, H., Zhang, J., Song, S., Wu, G., and Pu, J. (2011). Modified nanocrystalline cellulose from two kinds of modifiers used for improving formaldehyde emission and bonding strength of urea-formaldehyde resin adhesive. *BioResources* 6(4), 4430-4438.

Zivic, F., Grujovic, N., Adamovic, D., and Divac, D. (2017). Development of new composites made of waste Materials for wood pallet element. In Advances in applications of industrial biomaterials (pp. 201-214). Springer, Cham.

Article submitted: December 30, 2018; Peer review completed: ----------; Revised version received and accepted: ----------; Published: